ABSTRACT

CHAUDHARY, CHELSEA ERIN. Point Mutagenesis and Spectroscopic Probing of Dehaloperoxidase: Characterizing the Mechanism and Activity of the Heme Active Site of the Native Enzyme. (Under the direction of Stefan Franzen)

The research presented in this thesis focuses on DHP, the three mutants of DHP (Y39F, H56R, and H90G), and their relationship to well known enzymes such as HRP and myoglobin. Two methods of doing point mutations were performed on three DHP amino acids, which were near the active site and/or the heme, to understand more about the substrate binding activity and product formation of the native enzyme. Mutagenesis techniques employing the polymerase chain reaction (PCR), ligation, transformation, inoculation, and protein purification were carried out. Specifically, Y39F was developed due to its proximity to the substrate binding site and its hydrogen bond to the bound substrate. H56R and H90G are commonly studied mutants of myoglobin, which have been shown to decrease activity due to the changes in the R groups of the mutated amino acids. Activity assays for understanding the reaction of the heme in DHP were developed and performed on the native enzyme as well as Y39F, H56R, and H90G. The assays included using tri-halogenated phenols, hydrogen peroxide, and differing concentrations of enzyme in a pH 7 phosphate buffer. Spectroscopic probing on a multi wavelength ultraviolet/visible spectrometer revealed that all mutants and the native protein differ in the rate and amount of product formed as well as heme degradation (due to the peroxide). Singular Value Decomposition, SVD, calculations were carried out to single out the three components of the reaction (product growth, substrate consumption, heme shift and concentration change) and then the matrices were rotated by specified angles for further analysis.

POINT MUTAGENESIS AND SPECTROSCOPIC PROBING OF DEHALOPEROXIDASE: CHARACTERIZING THE MECHANISM AND ACTIVITY OF THE HEME ACTIVE SITE OF THE NATIVE PROTEIN

by

CHELSEA ERIN CHAUDHARY

A thesis submitted to the Graduate Faculty of
North Carolina State University
in partial fulfillment of the requirements
for the Degree of
Masters of Science

DEPARTMENT OF CHEMISTRY

Raleigh, North Carolina

May 2003

APPROVED BY:

Dr. Daniel L. Feldheim

Dr. Steven Lommel

Dr. Stefan Franzen
Chair of Advisory Committee

DEDICATION

This work is dedicated to my mother, Cindy Helen Dixon, who was a source of much encouragement throughout my high school and college years. This work is also dedicated to my father, Scott Lambert Dixon, whose devotion to my successful growth in life and his own work as a contractor has been an inspiration for my committed work habits.

BIOGRAPHY

Chelsea Erin Chaudhary was born in Douglasville Georgia September 10, 1978. In 1985 with her parents and brother, she moved to Cumming Georgia where she graduated from South Forsyth High School in 1996. She attended the University of West Georgia in 1996 in Carrollton Georgia where she majored in chemistry with a biochemistry emphasis and received her Bachelors of Science degree in May 2001. Chelsea immediately enrolled in the chemistry graduate program at North Carolina State University in Raleigh North Carolina. She married Kleem Chaudhary on June 29, 2002 in Chapel Hill North Carolina. Chelsea spent two years working on her Masters of Science degree in Chemistry.

ACKNOWLEDGEMENTS

Dr. Stefan Franzen

Dr. Tim Sit

Dr. Steven Lommel

Dr. Daniel Feldheim

Franzen Group

Research Funded by National Science Foundation

TABLE OF CONTENTS

LIST OF TABLES

Page

LIST OF FIGURES

Chapter 1: Introduction and Background

1.1 Introduction

A novel heme peroxidase known as dehaloperoxidase (DHP) was isolated from the marine worm *Amphitrite ornata*. The function of the enzyme DHP is a central target of the studies in this thesis. The spectroscopic studies of enzyme function described in this thesis were developed to understand the mechanism of DHP. The major tool used was the mutation of key amino acids that affect the heme active site or the binding pocket. Three mutants were created in this study and their activity was spectroscopically probed with a UV-vis spectrometer. Because of the complexity of the reactions, these mutants, DHP, and horseradish peroxidase (HRP) will be analyzed using Singular Value Decomposition (SVD). There were possible intermediates noticed by comparing the rate constants of product formation and substrate decrease. Many questions were revealed when, in DHP, the product was formed twice as fast as the substrate was consumed, leading to a hypothesis that there is a complex mechanism with intermediates involved and possible polymerization of the product. The SVD matrix was then analyzed using a rotational matrix procedure to understand more about DHP's mechanism of dehalogenating phenols. Because SVD did not make known answers to the questions by separating the components, rotational matrix manipulation was used to single out the 3 or 4 components of the reaction. The final results revealed clues to the possible intermediate/polymerized product formation in DHP.

The studies carried out in this thesis contribute to the practical application of a new type of peroxidase represented by DHP. The pulp and paper industry produces large quantities of waste from bleaching that is harmful to the environment. Though there are many efforts to try and change the way the industry dumps waste, another method is to

change the removal processing to avoid dumping toxic materials altogether. The concept of using a microorganism for an enzymatic process for environmental cleanup is known as bioremediation. There are many organisms as well as enzymes, particularly including dehalogenating peroxidases, that can be used for bioremediation. This study focuses on the enzyme dehaloperoxidase (DHP) from the marine worm *Amphitrite ornata*, which has unique potential for bioremediation. The uniqueness of DHP for the possible use in bioremediation is that it possibly binds oxygen as an oxygenase instead of peroxide which could be harmful to bacteria. The fold of DHP is that of a globin, but the dehalogenating activity is that of peroxidases.

1.2 Background

1.2.1 Bioremediation

Phenols are a general pollutant that happen to be a chemical waste material made by the bleach plant washer filtrates.[1] Faced with the problem of not knowing how chemicals affect the hydrosphere, Congress directed the U S Geological Survey (USGS) to conduct a program to provide this critically needed information in the 1980's.[2] This program was known as the Toxic Substances Hydrology Program. One of the principal findings of this program was that microorganisms in shallow aquifers affect the fate and transport of virtually all kinds of toxic substances. Most of the cost associated with traditional cleanup technologies is associated with physically removing and disposing of contaminated soils. Because engineered bioremediation can be carried out in place by delivering nutrients to contaminated soils, it does not incur removal-disposal costs and therefore is a favorable method. At some sites, natural microbial processes can remove or contain contaminants at a lower cost without human intervention.[2] The US EPA priority list of dangerous pollutants includes 11 phenols, including 2,4,6 trichlorophenol (TCP).[3] Bioremediation studies have focused on peroxidase enzymes as a strategy to break down phenols in the environment. Dehaloperoxidase from *Amphitrite ornata* is a peroxidase that has recently been characterized and has desirable properties that are significantly different from other known peroxidases such as HRP (Horseradish Peroxidase). One of these differences is that possibly it uses oxygen instead of peroxide as the cosubstrate as in oxygenases.

1.2.2 Heme Proteins: Structure and Function

1.2.2.1 Structure

An enzyme is a protein synthesized by a living cell, which catalyzes a specific reaction necessary for the maintenance of life. Unlike ordinary chemical catalysts, enzymes characteristically have the ability to catalyze a reaction under very mild conditions in neutral aqueous solutions at normal temperature and pressure, and with very high specificity. There are a number of enzymes that contain the heme cofactor, oxidases, peroxidases, mono- and dioxygenases, nitric oxide reductase and many more. Peroxidases have been studied since the early 1900's because of their ready extraction from plants and extraordinary reactivity with certain substrates. The first X-ray crystallographic structure of a protein was solved for the heme protein myoglobin in 1960 by John Kendrew. [4]

The heme prosthetic group serves as the ligand-binding site, the catalytic site, or the redox site in heme proteins. [5] The heme proteins studied in this thesis have the prosthetic group ferroprotoporphyrin IX containing iron (II) called heme. The name heme is used even though the oxidation state of the heme changes throughout the reaction. There are four methyl groups (positions 1, 3, 5, and 8), two vinyl groups (2 and 4), and two propionate groups (6 and 7). The official name of the porphyrin is 1,3,5,8-tetramethyl-2,4-divinylporphine-6,7-dipropionic acid. In the native enzyme, the resting state of heme proteins is most likely iron (III) five coordinate.[6]

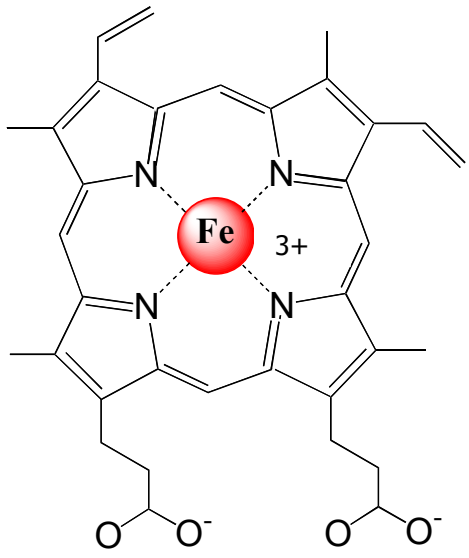

Figure 1.1 Heme iron(III) five coordinate

The peroxidase class of heme proteins has made a major contribution to the development of modern enzymology. In peroxidases, the heme iron is ligated in positions 1-4 which are the four pyrrole nitrogen atoms. In figure 1.1, one of the axial positions (Position 5) is occupied by a histidine strongly coordinated to the heme iron. The axial histidine is known as the proximal histidine. The histidine on the opposite side of the heme, where diatomic ligands and peroxide bind (Position 6), is known as the distal histidine. In the native state of peroxidases the distal histidine is not ligated to the heme iron. In reactions with substrates, the propionate side chains form hydrogen bonds with neighboring residues.

The distal cavity is the center of most activity in peroxidases. Diatomic ligands or peroxides enter and bind to the heme iron. The substrate must approach the heme active site either through a channel in the protein (horseradish peroxidase), a bound cytochrome c (cytochrome c peroxidase) or a substrate binding site (dehaloperoxidase from *A. ornata*). The control of reactivity is governed by the amino acid residues near the heme

iron that control proton transfer and electron transfer pathways to and from the active site. Dehaloperoxidase, a novel heme peroxidase, has only been studied in the past decade. DHP I from the marine worm, *Amphitrite ornate,* was cloned by Chen et al. DHP I is a heme enzyme (Mr = 30,790) composed of two identical subunits (Mr = 15,529) and is very rich in aspartic acid and glutamic acid residues.[7] The spectroscopic peak for heme is called the Soret band. The Soret band has characteristic wavelengths ranging from 380 – 440 nm for each of the states of HRP. The ferric resting state of HRP has a Soret band at 409 nm, while compounds I and II are observed at ~380 and ~421 nm, respectively.[9] in DHP the ferric and compound II bands absorb at the same wavelengths as the respective bands in HRP. Compound I has not yet been observed in DHP.

DHP has a homologous structure with members of the globin family, but the amino acid sequence identity is low. However, the structural differences between DHP and myoglobin are on the order of differences among globins.[8] Although the structure of DHP is like myoglobin, the mechanism and activity of the enzyme is more like HRP. It is shown by x-ray crystallography that peroxidase folds are different than globin folds. DHP has a globin fold and a peroxidase reactivity. HRP, like cytochrome c peroxidase (Ccp), has a distal histidine, whereas DHP has a distal valine. Histidine 56 in DHP is 9.1 Å away from the heme, whereas, the distal histidine 53 in CcP is 5.6 Å away and the distal histidine in HRP is 5.8 Å away from the heme. In DHP, it is proposed in this thesis that even though H56 is not the distal histidine, it is playing a major role in the mechanism for the enzyme reaction. HRP, a heme peroxidase, was being studied even before most enzymes were discovered. According to the x-ray crystal structure, HRP has a binding tunnel that allows the substrate to be exposed to buffer continuously. Whereas,

according to the x-ray crystal structure, dehaloperoxidase (DHP) has a binding pocket that allows no buffer to be exposed to the bound substrate.

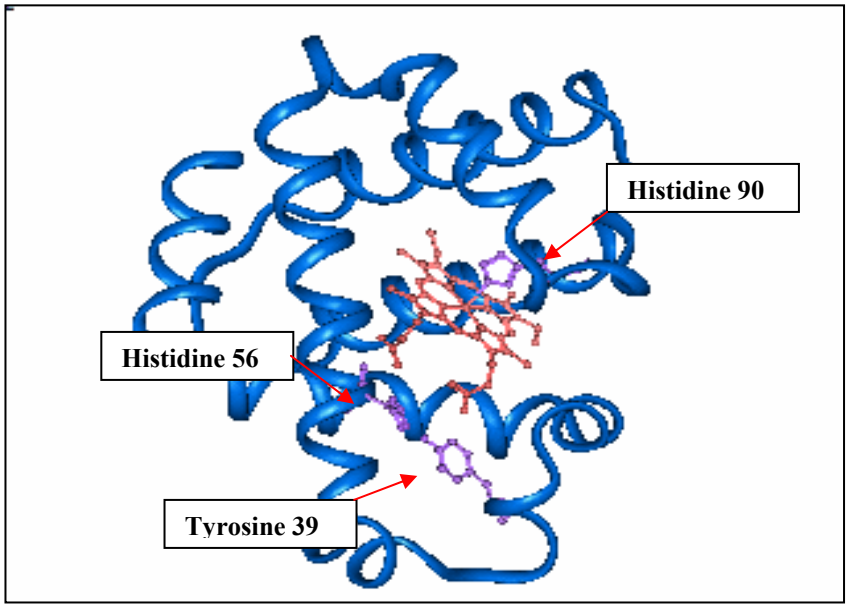

Figure 1.2 A model of the heme active site and binding pocket. The mutated amino acids are near the heme site.

1.2.2.2 Function

Peroxidases differ from most enzymes in that they do not bind substrates reversibly. For this reason the kinetic schemes for peroxidases do not follow Michaelis-Menton kinetics.[6] Most peroxidases, including HRP, follow this scheme for binding organic substrates and peroxide:

$$\text{HRP} + H_2O_2 \rightarrow \text{Compound I}$$

$$\text{Compound I} + X_3BOH \rightarrow \text{Compound II} + [X_3BO]\bullet + H^+$$

$$\text{Compound II} + X_3BOH \rightarrow \text{HRP} + [X_3BO]\bullet + H^+$$

Compound I is the oxoferryl form of the heme with a positive charge and compound II is the oxoferryl form of the heme with a phenol cation radical. There are two proposed mechanisms that occur in DHP and, for that matter, most peroxidases. The first mechanism is a one-electron process that is shown above and results in a polymeric product. This mechanism for polymerization involves the interaction of X3BO• with the phenolic substrate. The second mechanism that is possible is a two-electron process in which the substrate remains close to the heme iron so that the radical X3BO• is oxidized further to form a quinone product. Until recently, quinone was the only reported product for HRP in the dehalogenating reaction. It is interesting that both polymeric and quinone products have been found in the reaction of HRP with trihalogenated phenols in more recent reports. However, it has not been previously proposed that both mechanisms could occur at the same time.

DHP is a more perplexing enzyme because of the structural homology to myoglobin and the dehalogenating activity similar to many peroxidases. It is likely that the heme active site is responsible for the novel activity of DHP. The peroxide/substrate binding reaction is complicated in DHP because H_2O_2 can oxidize and degrade the heme to a much higher extent than in HRP. DHP has been found to be an unusual peroxidase, sometimes lending itself to be called a dehaloperoxygenase.[10] Peroxidases do not utilize the distal cavity as an organic substrate binding pocket, but rather the reaction takes place on the heme edge.[10] In DHP, it has been speculated, based on an x-ray crystal structure, that since the reaction does not take place at the heme edge like most peroxidases but in the distal pocket, that the intermediate does not carry the oxidative equivalent in the form of a porphyrin radical (compound I) as found in

peroxidases.[8] What was called the distal histidine in previous literature is being questioned in this thesis because of the large difference in the distance of H56 DHP and, for instance, H53 Cytochrome c peroxidase from the heme center. It was thought that DHP binds peroxide and uses the distal histidine as the pull to accomplish the heterolytic cleavage of the oxygen-oxygen bond.[8] This hypothesis is still supported in this study, but naming the histidine the 'distal histidine' is being refuted because the mechanism is thought to be different in DHP compared to other peroxidases. When the iron-oxo intermediate is ready, the distal histidine swings out of the cavity enabling the substrate to enter the distal pocket and undergo oxidation.[8] DHP was previously hypothesized to have a unique mechanism that uses an oxygen atom from peroxide that transfers to the substrate with oxidation of the aromatic substrate to a quinone product.[11] DHP oxygenates and dehalogenates halo aromatics and yet has a proximal histidine like many peroxidases that do not have this combined reactivity.[12] The known mechanism for peroxidases, the Poulos-Kraut mechanism, is likely the mechanism for DHP with some slight differences.

Myoglobin has been studied extensively by site-directed mutagenesis of the heme active site and, in fact, the entire protein. H93G is a key myoglobin mutant because of its removal of ligation by the proximal histidine that stabilizes and controls the heme reactivity.[13-18] The role of the proximal histidine in myoglobin can be assessed by replacing it with a noncoordinating residue to create a cavity where exogenously added ligands can bind and coordinate to the heme iron.[19-21] Imidazole can be added as an exogenous ligand that ligates the heme iron, but is not covalently bound to the protein. Exogenous imidazole is capable of rescuing the function of myoglobin to a large extent.

H93G(Im) with imidazole bound is capable of binding oxygen reversibly, however, with a reduced binding affinity.

Although it is not structurally related, cytochrome c peroxidase (CcP) is a model protein that can be used for functional comparisons with mutations of DHP. In particular, the proximal histidine mutant (H175G) of CcP has been extensively studied by Goodin and co-workers. In the case of CcP, chemical rescue is not possible. Exogenous imidazole only binds as imidazolate (protonated imidazole). In this form the enzyme is not functional. Thus, it is of interest to compare the proximal histidine mutant of DHP with those of Mb and CcP to understand the role played by the proximal histidine in DHP.

DHP can be compared to HRP in the activity studies presented in this thesis. Both DHP and HRP react with trihalogenated phenols and H_2O_2 to produce a product thought to be a dihalogenated quinone.[12] It has been found previously by UV-vis spectroscopy and gas chromatography-mass spectrometry that the product of the reaction with HRP and 2,4,6 trichlorophenol is 2,6-dichloro-1,4-benzoquinone.[3] HRP has a distal histidine that is involved in the reactivity of the heme because of its hydrogen bond with the bound peroxide as in the Poulos Kraut mechanism.

Poulos Kraut mechanism:

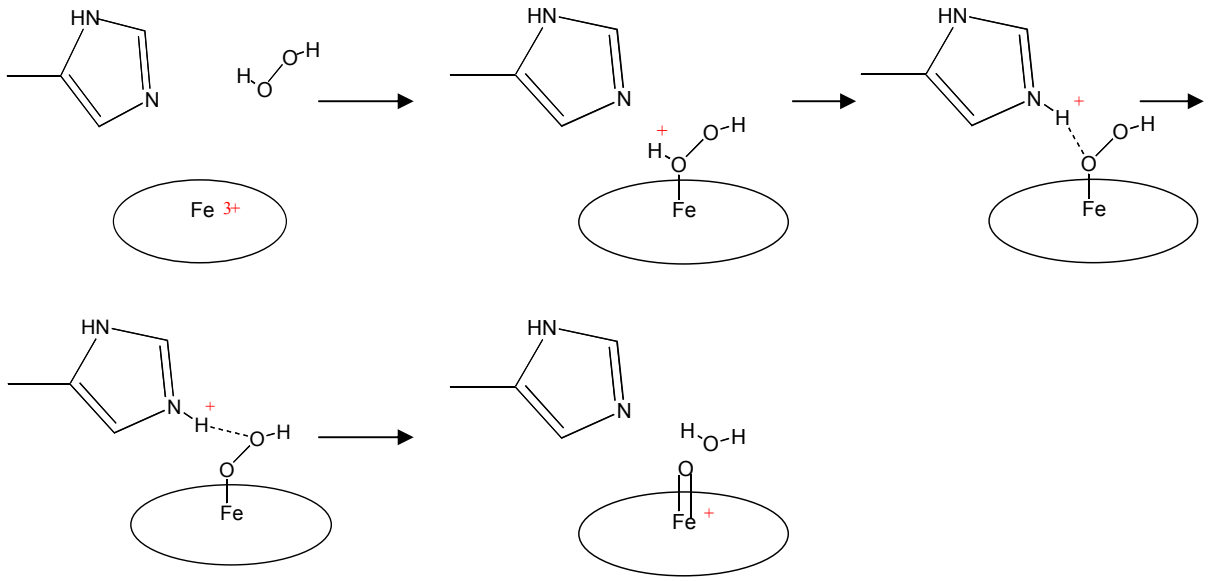

Dehaloperoxidase from *Amphitrite ornata* has only been studied in recent years and the research presented in this thesis is the first to study DHP mutants. To understand the role of key amino acids we have made three mutants of the enzyme Y39F, H56R, H90G. Mutagenesis of DHP has allowed more understanding of the native enzyme by targeting these activity relevant amino acids. The labeling system used for the DHP mutants was taken from the amino acid sequence which includes the start codon. In the crystal structure, the numbering of the residues is off by one because the start codon is not expressed as a residue. The histidine 56 was mutated in this study and the results support the former hypotheses that it is used in the Poulos Kraut mechanism acting as the distal histidine. One mutant was made because the well-known H93G myoglobin is an analogous mutant to H90G DHP. This mutant provides a key functional test of the nature of the enzyme. The proximal histidine is responsible for the "push" in the "push-pull" mechanism of peroxidases. The proximal histidine of DHP (H90) has been

formerly studied by resonance Raman spectroscopy to show that the Fe-N bond is stronger than in globins but not as strong as in peroxidases.[8] It has been previously stated that DHP appears to bind an organic substrate close to a very active oxygen atom and works without a system of complicated hydrogen bonds and other interactions that are characteristic of enzymes with more sophisticated mechanisms.[8] Because we have found that peroxide degrades the heme of DHP to a higher extent than other peroxidases, in this study, we will support the hypothesis that an oxygen is the native cosubstrate in the enzyme activity rather than hydrogen peroxide.

1.2.3 Mutagenesis

The three mutations of DHP that were made in this study are Y39F, H56R, and H90G. The tyrosine in the 39th position in DHP has been mutated to a phenylalanine to understand more about the binding pocket. This mutation was chosen due to its proximity to the binding pocket and because of the hydrogen bond that it appears to make with the hydroxyl group of the phenolic substrate in the x-ray crystal structure. The histidine in the 56th position in DHP has been mutated to an arginine to be compared with the similar mutant of HRP. In HRP this histidine is the distal histidine to the heme and plays a key role in the efficiency of the iron state and mechanism. The histidine in the 90th position in DHP has been mutated to a glycine, which was compared to the well-known myoglobin mutant H93G and the well-known CcP mutant H175G.[13-18] This mutation affects the proximal histidine, which is a key player in the iron oxidation state. The charge on the histidine determines the possible oxidation states of the iron and thereby controls the reactivity of the iron in the oxygen scission required for peroxidase function. The amino acid changes are shown below in the protein sequence of DHP.

DHP Protein Sequence with Mutations:

F
GFKQDIATIRGDLRTYAQDIFLAFLNKYPDERRYFKNYVGKSDQELKSMA
R G
KFGDHTEKVFNLMMEVADRATDCVPLASDANTLVQMKQHSSLTTGN

FEKLFVALVEYMRASGQSFDSQSWDRFGKNLVSALSSAGMK

Shown Above: In Blue are the native amino acids that were mutated.
In Red are the single point mutations made to form each mutant.

Site-directed mutagenesis of an enzyme is the purposeful alteration of one amino acid to study or change the inherent mechanism of the enzyme. Modern application of site-directed mutagenesis uses the Polymerase Chain Reaction (PCR) as the central method for generation of an altered DNA sequence for incorporation into plasmid DNA. PCR was developed in 1985 by Kary B. Mullis and others. In PCR, DNA is dissolved in a solution containing the enzyme DNA polymerase, oligonucleotides, and "primers," short sequences of nucleotides designed to bind with an end of the desired DNA segment. Two primers are used: one primer binds at one end of the desired segment on one of the two paired DNA strands, and the other primer binds at the other end but on the other strand. To achieve mutagenesis of the entire DNA, one and/or two of the primers will have the mutation in it/them. The solution is heated to break the hydrogen bonding between the strands of the DNA. When the solution cools, the primers anneal to the separated strands, and DNA polymerase quickly synthesizes a new strand by joining the free nucleotide bases to the primers. When this process is repeated, a strand that was formed with one primer anneals to the other primer, resulting in a new strand that is restricted solely to the desired segment. Thus the region of DNA between the primers is

selectively replicated. Further repetitions of the process can produce billions of copies of a small piece of DNA in several hours with the enzyme Taq Polymerase.[22]

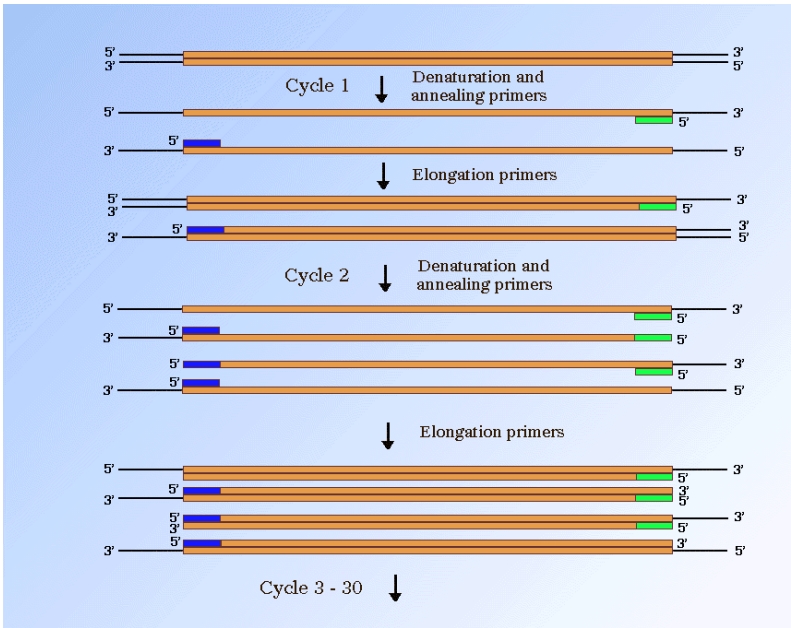

Figure 1.3 Representation of the Mechanism of Polymerase Chain Reaction

After determining the PCR reactions occurred with high-fidelity by running an electrophoresis gel of the PCR product, plasmid DNA from the DHP pET16b strain was isolated by phenol-chloroform extraction. A double digest was performed for the ligation of the fragments. Once the ligation reactions of the pcr product with a linearized bacterial plasmid were completed, the products were transformed into competent bacterial cells. H90G and H56R mutations were created by a different mechanism and this process is described in the next chapter.

1.2.4 Spectroscopic Assay for DHP Function

The dehalogenating reaction of the enzyme was studied and contained peroxide, trihalogenated phenols, and enzyme in buffer. Spectroscopic probing of the reaction was conducted to understand the conversion substrate to product. Also, the Soret band, which

contains information about the heme active site, was monitored. This assay is based on the knowledge that peroxide binds to the enzyme and allows it to bind the trihalophenol substrate. The enzymes studied then produce a product at various rates.

We obtained a data set that consisted of wavelengths vs. time. Fitting any particular wavelength to an exponential function gives a different result from any other wavelength, so a global fitting procedure was needed since there are multiple events happening in the reaction. The events happening are substrate decay, product formation, and heme degradation. It is assumed that as the UV-vis absorbance band correlated to the heme decreases over time with peroxide, the heme is being degraded. Singular value decomposition (SVD) was used as the global fitting procedure to separate out the different components of the reaction.

1.2.5 Singular Value Decomposition

Singular value decomposition (SVD) is a technique employed to analyze multivariate data. SVD was used to analyze the kinetics of the reactions. When performing SVD, a data matrix consisting of objects and variables is used. Objects are denoted with the subscript n, where n reresents the number of rows in the data matrix. Objects are simply varying or replicate samples. Variables are along each column, m, in the data matrix. Variables can be related to the concentration of constituents in a sample, such as peak height and area. Other variables such as electrochemical measurements, rate constants, refractive indices, and thermodynamic data can be utilized.[23] Spectral data is commonly digitized, thus, each wavelength or wavenumber is a variable.[24] When choosing variables, it is significant that the given variables pertain to all objects in the data matrix and one variable can represent more than one feature.

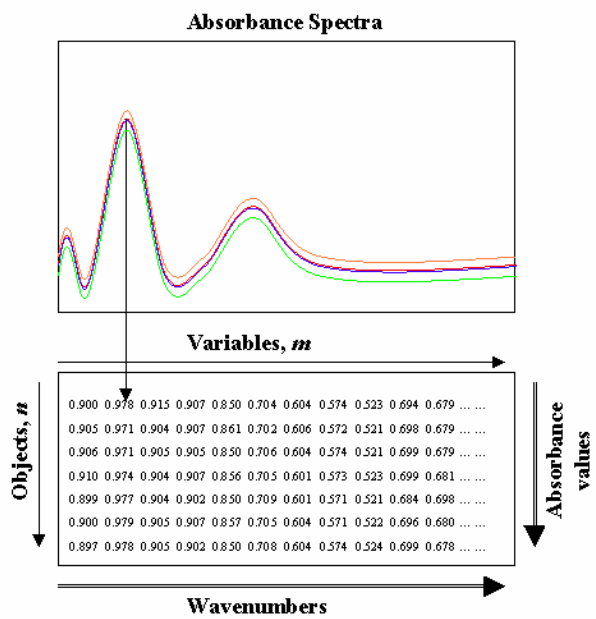

Figure 1.4 Schematic of digitized spectral data

The goal of SVD is to determine relationships between objects and variables in a data set.[23] The data matrix is of high dimensional space that is difficult to visualize. The method of SVD reduces the data set to a lower dimensional space. Data reduction is achieved by decomposing the data and discarding insignificant principal components. The term principal component can be thought of as a dimension or a factor. In some cases, factors represent real chemical properties.[24] In the following example, the data matrix has a row for each sample and a column for each wavelength. The number of eigenvectors generated is dependent upon n or m whichever is smaller.[24] Each eigenvector has an eigenvalue, which is the measure of importance of the associated eigenvector. The eigenvector associated with the largest and most important eigenvalue, in a least-squares sense has the greatest possible variance in the data. The data matrix is decomposed into a matrix of column mode eigenvectors, **U**, the singular values, **S**, and the row mode eigenvectors, **V**, by the singular value decomposition

function where **D** represents the data matrix. This method rotates the data in multidimensional space in order to align the linear combinations of the original data with the direction of the most variance.

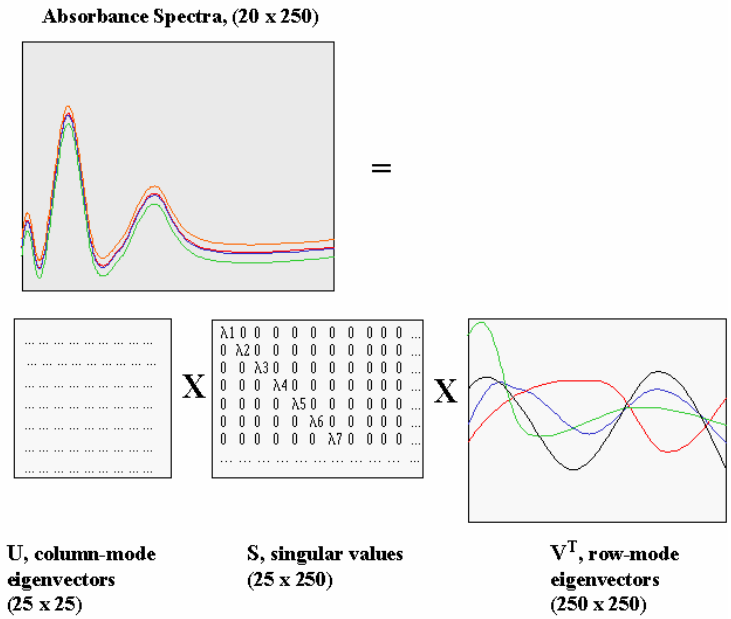

Figure 1.5 Representation of the singular value decomposition function for a (25 x 250) data matrix. [25]

A rotational matrix method was performed to further understand the link between heme degradation and activity

1.2.6 Rotational Matrix Method

A rotational matrix procedure has been performed on the SVD analysis data to separate out the components of the reaction. The product growth, substrate decrease, and heme shift and decrease is better understood by rotating the eigenvectors given in SVD analysis. Rotation of a matrix is defined by considering the singular value decomposition $\mathbf{A} = \mathbf{U}\ \mathbf{S}\ \mathbf{V}^{\mathbf{T}}$, and so then considering a rotation of the $\mathbf{V}^{\mathbf{T}}$ matrix as a mixing of the components. The transformation: $\mathbf{R}\ \mathbf{V}^{\mathbf{T}} = \mathbf{V}^{\mathbf{T}\prime}$. Then rotate the U matrix as $\mathbf{U}\ \mathbf{R}^{-1} = \mathbf{U}'$.

Here $\mathbf{R}^{\mathbf{T}} = \mathbf{R}^{-1}$ since R is a unitary matrix. The rotation matrix R can be expressed in terms of the angle θ.

$$R = \begin{pmatrix} \cos\theta & \sin\theta \\ -\sin\theta & \cos\theta \end{pmatrix}$$

The inverse matrix is:

$$R^{-1} = \begin{pmatrix} \cos\theta & -\sin\theta \\ \sin\theta & \cos\theta \end{pmatrix}$$

Using a rotation angle of θ it is found that the original components can be rotated to form linear combinations that represent distinct processes.

1.3 Scope

The research presented in this thesis focuses on DHP, the three mutants of DHP (Y39F, H56R, and H90G), and their relationship to well known enzymes such as HRP and myoglobin. Two methods of doing point mutations were performed on three DHP amino acids, which were near the active site and/or the heme, to understand more about the substrate binding activity and product formation of the native enzyme. Mutagenesis techniques employing the polymerase chain reaction (PCR), ligation, transformation, inoculation, and protein purification were carried out. Specifically, Y39F was developed due to its proximity to the substrate binding site and its hydrogen bond to the bound substrate. H56R and H90G are commonly studied mutants of myoglobin, which have been shown to decrease activity due to the changes in the R groups. Activity assays for understanding the reaction of the heme in DHP were developed and performed on the native enzyme as well as Y39F, H56R, and H90G. The assays included using tri-halogenated phenols, hydrogen peroxide, and differing concentrations of enzyme in a pH 7 phosphate buffer. Spectroscopic probing on a multi wavelength ultraviolet/visible spectrometer revealed that all mutants and the native protein differ in the rate and amount of product formed as well as heme degradation (due to the peroxide). Heme degrading and protein concentration varying studies helped to conclude the unusual activity of DHP. Singular Value Decomposition, SVD, calculations were carried out which allowed one to diagnose any problems in a data set by linearizing the eigenvectors of the spectra. The SVD analysis was carried further to single out the three components of the reaction (product increase, substrate decrease, heme shift and concentration change) by rotating the matrices by specified angles.

References:

[1] http://sunsite.nus.edu.sg/apcel/dbase/laos/regs/ladwwat.html

[2] http://water.usgs.gov/wid/html/bioremed.html

[3] R. P. Ferrari , E. Laurenti , F. Trotta. Oxidative 4-dechlorination of 2,4,6-trichlorophenol catalyzed by horseradish peroxidase. *Journal of Biological Inorganic Chemistry* **1999**, Volume 4, Issue 2, pp 232-237.

[4] J.C. Kendrew, R.E. Dickerson, B.E. Strandberg, R.G. Hart, D.R. Davies, D.C. Philips. Shore Structure of myoglobin: A three dimensional fourier synthesis at 2 Å resolution. *Nature* **1960**, 185, 422-427.

[5] T. K. Das, S. Franzen, A. Pond, J. H. Dawson, D. L. Rousseau. Formation of a five-coordinate hydroxide-bound heme in the His93Gly mutant of sperm whale myoglobin. *Inorganic Chemistry* **1999**, *38*, 1952-1953.

[6] H.B. Dunford. Heme Peroxidases. *John Wiley & Sons, Inc*. **1999,** Chapter 1.

[7] Y.P. Chen, S.A. Woodin, D.E. Lincoln, C.R. Lovell. An unusual dehalogenating peroxidase from the marine terebellid polychaete *Amphitrite ornata*. *Journal of Biological Chemistry* **1996**, 271, 4609-4612.

[8] M.W. LaCount. The Crystal Structure and Amino Acid Sequence of Dehaloperoxidase from *Amphitrite ornata* Indicate Common Ancestry with Globins. *The Journal of Biological Chemistry*, June 23, **2000**, vol 275, no. 25, 18712-18716.

[9] D. Keilin and T. Mann. *Proc. Roy. Soc. (London)* **1937,** 122B, 119-133.

[10] M.A. Ator and O.D. Montellano. Protein control of prosthetic heme reactivity. Reaction of substrates with the heme edge of horseradish peroxidase. *J. Biol Chem*. **1987** 262, 1542-1551.

[11] S. Kobayashi, M. Nakano, T. Goto, T. Kimura, A.P. Schaap. *Biochem. Biophys. Res. Commun*. **1986** 135, 166-171.

[12] M.P. Roach, The unusual reactivities of *Amphitrite ornata* Dehaloperoxidase and *Notomastus lobatus* Chloroperoxidase do not arise from a histidine imidazolate proximal heme iron ligand. *Biochemistry* **1997**, 36, 2197-2202.

[13] S. Franzen, B. Bohn, C. Poyart, G.D. DePillis, S.G. Boxer, J. Martin. Functional Aspects of Ultra-Rapid heme Doming in Hemoglobin, Myoglobin, and the Myoglobin Mutant H93G. *J. Biol. Chem*. **1995**, 270, 1718-1720.

[14] S. Decatur, S. Franzen, Dyer. Trans effects in nitric oxide binding to myoglobin cavity mutant H93G. *Biochemistry* **1996**, 35, 4939-4944.

[15] T,K. Das, S. Franzen, Formation of a five-coordinate hydroxide-bound heme in the His93Gly mutant of sperm whale myoglobin. *Inorg. Chem*. **1999**, 38, 1952-1953.

[16] S. Franzen, S. G. Boxer. Resonance Raman Studies of Heme-Axial Ligation in H93G Myoglobin. *J. Phys. Chem. B*, **2000**, 104, 10359-10367.

[17] S. Franzen, J. Bailey. A Photolysis-Triggered Heme Ligand Switch in H93G Myoglobin. *Biochemistry*, **2001**, 40, 5299-5305.

[18] M.R. Thomas, D. Brown. FTIR and Resonance Raman Studies of Nitric Oxide Binding to H93G Cavity Mutants of Myoglobin. *Biochemistry*, **2001**, 40, 15047-15056.

[19] D. Barrick. Replacement of the Proximal Ligand of Sperm Whale Myoglobin with Free Imidazole in the Mutant His-93->Gly. *Biochemistry* **1994**, 33, 6546-6554.

[20] G.D. DePillis, S.M. Decatur, D. Barrick, S.G. Boxer. Functional cavities in proteins: A general method for proximal ligand substitution in myoglobin. *J.Am.Chem.Soc*. **1994**, 116, 6981-6982.

[21] S.M. Decatur, S. Franzen, G.D. DePillis, R.B. Dyer, W.H. Woodruff, S.G. Boxer. Trans effects in nitric oxide binding to Myoglobin cavity mutant H93G. *Biochemistry* **1996**, 35,4939-4944.

[22] http://www.encyclopedia.com

[23] B.R. Kowalski, Chemometrics: Mathematics and Statistics in Chemistry. *D. Reidel Publishing Company*.**1983**, 17-48.

[24] E.R. Malinowski. Factor Analysis in Chemistry. *John Wiley and Sons, Inc*. **1991**, 1-71.

[25] Gemperline, P., *Chemometrics Short Course*, **1997.**

Chapter 2: Methods

2.1 Introduction

This chapter describes the materials and methods used in the study of DHP and three site specific mutants. The methods have been applied to obtain an understanding of the reactivity of the heme site, the dynamics of the binding pocket, and the mechanisms of enzyme activity. Two specific methods of mutagenesis (by a PCR method and a mutagenesis kit) and the purification of the proteins will be explained first. Second, the spectroscopic assay for enzyme activity will be discussed. Finally, the third section will explain the methods used to reduce the spectroscopic data by SVD and a matrix rotation procedure.

2.2 Mutagenesis of DHP to H56R, Y39F, and H90G

2.2.1 Introduction

Mutagenesis of DHP will enhance our understanding of the native enzyme function by targeting three key amino acids relevant to activity. The three mutants made are Y39F, H56R, and H90G. This section focuses on how and why these mutations were made. The same method of mutagenesis was used on H56R and H90G and therefore, they share a section of this chapter. They also will be shown in the same electrophoresis gels. The mutations included the amino acid change and also a change to incorporate a restriction site for test digestion that did not change that particular amino acid.

2.2.2 Materials

The N-terminal 6xHis DHP Pet 16b expression vector was supplied by Jennifer Belyea. This construct was the parental clone for all DHP mutants. All the primers used in the PCR reactions were ordered from Sigma-Genosys The Woodlands, TX. The restriction enzymes were from New England Biolabs Beverly, Mass. Qiagen provided the Qiagen miniprep kits and the Nickel NTA beads for protein purification (Qiagen, Valencia, CA). Mutagenesis was performed using the QuikChange® Site Directed Mutagenesis Kit (Stratagene Lajolla, Ca.). Novagen provided the E. coli Rosetta™ competent cells. Promega provided the 100mM dNTPs (Madison, Wi). The thermocycler was a Stratagene Robocycler Gradient 96. New Brunswick Scientific Company Inc. Edison, NJ makes the shaker incubator used. DNA was quantified on the Bio-Rad Spec3000 Bio-Rad Laboratories Hercules, Ca. The sequencing was done by MWG Biotech Inc. High Point, NC. The TB broth and the nickel sulfate solution was

from Fischer. The LB broth was from Sigma Ronkonkoma, NY. The centrifuge used for purification of the proteins was a Sorvall® SS-34 Newtown, CT.

2.2.3 Mutagenesis of DHP to Y39F DHP

General DNA manipulations were performed according to Mittal et. al. (2000).[1] Mutant Y39F was prepared by in vitro mutagenesis of DHP using the megaprimer method (Sarkar and Sommer, 1990).[2] Each reaction contains 10mM dNTPs, 10pmol/µl 5' primer, 10pmol/µl 3' primer, 10x polymerase buffer, 25mM $MgCl_2$, 1ng/µl DNA, 2.5U/µl Pfu Turbo polymerase, and water to bring the final volume to 50µl. The 5' primer was 6x His DHP+, and the 3' primer was Y39F-.

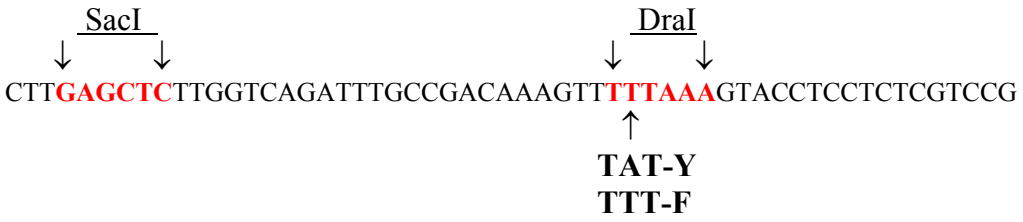

Figure 2.1 Y39F- primer sequence with restriction sites and mutation site are in red. Mutation site codes for a Phenylalanine(F) previously coding for a Tryptophan(Y)

The reactions were vortexed and transferred to small pcr tubes (50µl reactions). The three tubes were positioned in the thermocycler at 54º, 56º, and 58ºC annealing temperatures. They were denatured at 94° C for 1 minute for 2 cycles and 45 seconds for 38 cycles. They were annealed at the temperatures previously mentioned for 1 minute for 2 cycles and 45 seconds for 38 cycles. The extension was 72°C for 1.5 minutes for 2 cycles, 1 minute for 38 cycles, and 10 minutes for 1 cycle. The pcr products were run on an agarose DNA gel to see the new DNA band.

After determining the reaction followed through properly, the three tubes were pooled together and phenol chloroform extracted. One volume of phenol chloroform was added to the pooled DNA and it was vortexed. It was then centrifuged at 13,200 rpm for 2 minutes. The top layer, the aqueous phase, was placed in a new tube labeled #1. 100µl of TE buffer was added to the organic phase, vortexed, and centrifuged for 2 minutes. The new aqueous phase was removed and added to tube 1. One volume of chloroform was added to tube 1, vortexed, and then centrifuge for 2 minutes. The aqueous phase was removed and added to a new tube labeled 2. 1/10 of the volume of sodium acetate was added to tube 2 and vortexed slightly. 2 ½ volumes of 95% ethanol were added and the tube was inverted to mix. The tube was stored in –20°C for 15 to 20 minutes. The sample was centrifuged at 12,000 rpm for 5 minutes. The supernatant was discarded and the sample pellet was cleaned with 300µl of 70% ethanol. The sample was dried by speed vacuum for 5 minutes.

The PCR fragment and the pET16b plasmid vector were digested with restriction enzymes. The restriction enzymes chosen to ligate the Y39F insert to the vector were at the 5' end, NcoI, and at the 3' end, SacI. A double digest was performed for the ligation of the fragment. The digest of the insert contained 20µl of DNA, 5µl of 10xNEB1 buffer, 0.5µl of BSA, 24.5µl of H2O, 3µl of NcoI (10units/µl), and 1.5µl of SacI (20units/µl). The digest for the vector was the same as the previous except it contained 30µl of DNA (vector PET 16b) and 14.5µl of H_2O. These amounts were determined based on visual estimation of EtBr stained samples in an electrophoresis gel. The darker the band, the more concentrated the sample. A one-to-three ratio of vector and insert needed to be achieved. A control was run without the restriction enzymes. All of the

digests were incubated at 37°C for 2 hours and stored in –20°C. The products of the digests were run on an electrophoresis gel and using a Qiagen kit, Y39F was gel purified. Another gel was run of the purified samples to make sure there were no alterations to the samples during purification.

The ligation of the insert to the vector required a ligation reaction containing 1µl of the Y39F insert, 1µl vector, 1µl buffer, 1µl ligase, and 6µl H_2O. The controls that were run had no fragment or had no ligase. The reactions were vortexed, spun down for a few seconds in a centrifuge, and put in a 16°C water bath overnight.

Once the ligation reactions were finished the products were transformed into competent E. coli DH5α cells. 10µl of DNA ligation mixture was added to the cells (one ligation reaction per tube of cells) and they were gently vortexed. The tubes were incubated on ice for 15 minutes and then heat shocked at 42°C for 2 minutes. 400µl of LB broth containing 20mM glucose was added to the tube and then it was mixed gently by inversion and incubated at 37°C for 20min. After incubation, the culture tube was gently re-mixed by inversion and 125µl of the culture was pipetted onto one ampicillin LB Agar plate and the remainder (about 375µl) was pipetted onto the second plate. The plates were placed into a 37°C incubator to let the bacteria grow overnight.

Methylated DNA was prepared from *E. coli* DH5α cells by the mini alkaline lysis procedure. A single ligation colony was inoculated in 3ml of TB broth overnight with 75µg/ml of ampicillin. 1.5ml of the overnight bacterial culture was transferred into a microfuge tube and pelleted at 12,000 rpm for 35 seconds. The supernatant was decanted and the pellet was stored at –20°C/-70°C for a minimum of 10 minutes. The pellet was thawed for a few minutes at room temperature and then resuspended in 150µl of Solution

I (25mM Tris-HCl pH 8.0, 10mM Na_2 EDTA, 50mM dextrose (D-glucose), 3 mg/ml lysozyme) by vigorous vortexing. 300µl of Solution II (0.2N NaOH, 1% SDS) was added and the tube was mixed gently by inversion until the cell suspension cleared. 250µl of Solution III (3M NaAc pH 4.8) was added and the tube was mixed by inversion until no traces of yellow liquid remained (chromosomal DNA appeared). The tube was incubated on ice for a minimum of 15 minutes. The chromosomal DNA was pelleted at 12-13,000 rpm for 10-12 minutes. The supernatant was transferred into a new 1.5ml tube and 1 volume of cold isopropanol was added. The tube was incubated on ice for 5-10 minutes (or at –20°C indefinitely).

A test digest was performed on the Y39F DHP DNA to confirm the existence of the mutant DNA by verifying the new restriction site. The mixture contained 2µl of Y39F DNA, 1µl of DraI, 2µl of buffer, and 15µl of H_2O. The mixture was vortexed, spun down, and incubated at 37°C for 1 hour. An electrophoresis gel was run on the test digest and it shows that there was excess RNA in the plasmid preparation and this was removed. One volume of 5M ammonium acetate was added to DNA solution. The tube was mixed by vortexing and it was incubated on ice for 20 minutes. The tube was centrifuged for 10 minutes at 13,000 rpm to pellet the precipitate. The supernatant was transferred to a new tube and 2 volumes of cold 95% EtOH were added. The DNA was precipitated at –20°C for 15 minutes. The DNA was pelleted at 12,000 rpm for 5 minutes. The supernatant was discarded and the pellet was washed with 300µl 70% EtOH. Then the pellet was vacuum dried for 3-5 minutes and resuspended in 50µl of TE buffer with a pH of 8.0. Y39F DNA #2 and #4 were transformed into DH5α cells and plated on LB plates with ampicillin.

To sequence the DNA, it was purified with a Qiagen Miniprep Kit. Y39F #2 and #4 DNA were transformed into the *E. coli* Rosetta™ (DE3) plysS cell line to express the protein. Chloramphenicol was added to the agar plates and they were incubated overnight. Colonies picked off of the plates were inoculated overnight in 3mL of TB broth in a shaker at 37°C. Ampicillin, chloramphenicol and imidazole (40mg/ml) were also added to the overnights. The next day the cell culture was transferred to 400-500ml of LB broth with the antibiotics and imidazole and incubated in the shaker for 6 hours. The inoculation was removed and centrifuged for 20 minutes at 15,000 rpm. The cell pellet was removed and stored at –20°C. The pellet was light red and turned redder as the days progressed.

2.2.4 Mutagenesis of DHP to H56R DHP and H90G DHP

Because of unknown errors, the H56R and H90G could not be mutated by PCR like Y39F, consequently, another method was employed. The QuikChange® Site-Directed Mutagenesis Kit was used to mutate DHP into H56R and H90G. Each reaction contains 10mM dNTPs, 10pmol/μl 5' primer, 10pmol/μl 3' primer, 10x polymerase buffer, 25mM $MgCl_2$, 1ng/μl DNA, 2.5U/μl Pfu Turbo polymerase, and water.

SacI PvuI

H56R(+) CAAGAGCTCAAGTCAATGGCCAAGTTCGGCGATCGCACTGAGAAGTGTTCAACC

CAC-H
CGC-R

H56R(-) GTTCTCGAGTTCAGTTACCGGTTCAAGCCGCTAGCGTGACTCTTCACAAGTTGG

XhoI

H90G(+) CACTCGTCCAGATGAAACAGGGCTCGAGCCTGACGACTGGAAACTTC

CAT-H
GGC-G

H90G(-) GTGAGCAGGTCTACTTTGTCCCGAGCTCGGACTGCTGACCTTTGAAG

Figure 2.2 H90G and H56R forward and reverse primer sequences. The restriction sites are in red with the restriction enzymes above. The mutated sites are shown.

The reactions were aliquoted into 3 thin walled pcr tubes per enzyme to have a range of concentrations of DNA. The thermocycler setting for denaturation was 95° C for one cycle for 30 sec. The second set went for 16 cycles at 95° C for 30 sec, 55° C for 1 min., 68° C for 11.4 min. The third set, the extension, went for 11.4 min at 68° C.

The products were digested with 1µl DpnI restriction enzyme each and the mixture was pipetted up and down to mix. DpnI has a mechanism that only cleaves methylated DNA. The DNA produced from the previous thermocycling was not methylated because it was not put into *E. coli* and therefore, it will be the only DNA left. The digestions were centrifuged for 1 minute and incubated at 37°C for 1 hour immediately. The digestions were transformed into competent *E coli* DH5α cells and plated onto agar plates containing 100µg/ml ampicillin and incubated at 37°C overnight.

Inoculations of one colony per 3 mL of TB broth with 2.5µl of ampicillin were grown overnight in a shaker at 37°C. From these overnight cell growths, the plasmid purification kit was performed. Each mutant was test digested with a certain restriction enzyme to make sure the mutants were made. The restriction enzyme for H90G was xho1, and the restriction enzyme for H56R was pvu1. The reaction ingredients for the H90G digest were 12.5µl of H_2O, 5µl of DNA, 0.2 µl of BSA, 2µl of buffer, and 0.3µl of xho1. The reaction ingredients for the H56R digest were 12.3µl of H_2O, 5µl of DNA, 0.2µl of BSA, 2µl of 3Buffer, 0.5µl of pvu1. The control reactions had no restriction enzymes.

2.2.5 Protein Purification

For the mutants H56R and H90G, a heme addition was required because the heme was not in the *E. coli* expressed protein.[3] The pellet was resuspended in a minimal amount of lysis buffer and 40 µl of heme solution per gram of original cell pellet. This was allowed to stir for 30 minutes at 4°C. After stirring with the heme solution, the pellet was sonicated in an ice water bath for 30 minutes. After sonication, the pellet solution was centrifuged for 25 min. at 26,000 x g. The supernatant was collected and 10 µl of heme solution per gram of original cell pellet(10 mg heme/ml of 0.1 M NaOH) was added. This was allowed to stir at 4°C for 1 hour. After the supernatant finished stirring, it was centrifuged for 15 minutes at 26,000 x g. The supernatant of both solutions were combined. The combined supernatant solution was dialyzed in lysis buffer. The DHP solution was centrifuged for 15 min. at 26,000 x g. The supernatant was collected and pH of 6.0 was confirmed. The supernatant was loaded onto the column which is described below.

Cloned DHP from Rosetta™ (DE3) pLysS and DHP mutant Y39F were purified under native conditions. The purification of the 6X His tagged proteins were done using Ni-NTA agarose beads on a column. The procedure was modified from Qiagen's manual that accompanies the Ni-NTA agarose. The cell pellet was removed from –20°C and allowed to thaw in a 50 ml centrifuge tube with 10 ml of lysis buffer (50 mM NaH_2PO_4, 300 mM NaCl, 10 mM imidazole, pH 8.0) per gram wet weight of cell pellet for 15 minutes. Once cells were thawed they were resuspended by stirring at 4°C for 10 minutes. Once the cells were resuspended and lysozyme was added to a final concentration of 1 mg/ml, it was incubated on ice for 30 min. Then the cell mixture was sonicated in a water bath style sonicator for 30 min at 0°C. The lysate was very viscous, thus RNase A was added to a final concentration of 10 µl/ml and DNase I was added to a final concentration of 5µl/ml. This was allowed to incubate on ice for 15 minutes. The lysate was centrifuged at 10,000 x g for 30 minutes at 4°C (in 50 ml centrifuge tubes).

The translucent red lysate was loaded onto the column. The flow through was also translucent with an orange tint. When the lysate was loaded and the wash buffer (50mMNaH_2PO_4, 300 mM NaCl, 250 mM imidazole, pH 8.0) was applied at 3 times the column volume. The elution buffer (50 mM NaH_2PO4, 300 mM NaCl, 250 mM imidazole, pH 8.0) was added to the column next. Fractions were collected according to the intensity of the color of the eluted protein solution. The more red the fraction the greater the presence of DHP. Once the column was completely eluted the fractions were analyzed by UV-vis spectroscopy. Fractions that had high 415nm/280nm ratio wavelengths were used in assays.

2.3 Enzyme Assays

2.3.1 Introduction

Because DHP can be structurally compared to myoglobin, the basis for these assays come from known experiments done on myoglobin. Spectroscopic probing of the reaction will be conducted to understand the appearance of product and the disappearance of substrate. Also, the Soret band, which contains information about the heme active site, will be monitored. This assay is based on the knowledge that peroxide will bind to the enzyme and allow the enzyme to bind the trihalophenol substrate. The enzymes studied will then form a product at various rates.

2.3.2 Materials

Hewlet Packard 8453 multi-wavelength spectrometer was used for spectroscopic probing of the reaction. Acros Organics supplied all the tribromophenol, trichlorophenol, and trifluorophenol. Fischer provided the hydrogen peroxide. The potassium phosphate used to make the buffers was from Sigma and Fischer. The proteins were previously purified by methods already mentioned. The samples cells used were all 1cm path length quartz cuvettes.

2.3.3 Spectroscopic Assay for DHP Function

After purification on a Ni-NTA agarose bead column, DHP was concentrated in a centricon spincolumn and put into a centrifuge for spinning at 9,000rpm until the right concentration was achieved. The protein was then put into a solution of pH 7 10mM potassium phosphate buffer and placed into a cuvette for UV-vis spectrometer analysis. The Hewlet Packard 8453 multi-wavelength spectrometer was used to observe the peaks of interest. The concentration of DHP was determined by the absorbance of the Soret

band at 409nm, which is where the heme absorbs light. The extinction coefficient used for DHP is 188,000$M^{-1}cm^{-1}$, which is the extinction coefficient for myoglobin with CO bound. Once the absorbance of 0.113 was achieved, the substrate was mixed in the cuvette. Using Beer's Law, A=EbC, the concentration of all enzymes in each assay was calculated to be 0.601μM. The substrate was made by first dissolving a trihalogenated phenol in the 10mM potassium phosphate buffer to a certain concentration because it has low solubility. The final concentrations of tribromophenol and trichlorophenol were 98μM and the trifluorophenol concentration was 720μM. (Substrate:Enzyme=164:1) In one of the assays, the trichlorophenol concentration was decreased by ½ to 49μM. The spectrometer computer program HP 845x UV-Visible System was used to do a kinetics method once the hydrogen peroxide was added. The first spectrum taken contained no peroxide, then the hydrogen peroxide was added at a final concentration of 9μM, mixed, and every 3 seconds a spectrum was taken until 334 spectra resulted. The data was exported to Microsoft Excel and Igor Pro for analysis. Plots were made of absorbance vs. time for specific wavelengths related to product, substrate, or heme. These were fit by non-linear least squares fitting.

2.4 Analysis

2.4.1 Materials

The software package, MATLAB® v. 5.3 was used to perform SVD analysis on the kinetic data. Once the analysis was done, the program Igor Pro was used to display the data and to perform a rotational matrix procedure. Igor Pro was used to perform non-linear least squares fitting.

2.4.2 SVD Analysis and Rotational Matrix Procedure

After the kinetics were done on the UV-vis program, each spectrum was exported as a csv file into Microsoft Excel. The spectra were truncated to include one substrate peak, the product peak, and the Soret band. Also, around 30 time points were used for SVD analysis. The spectra were then loaded into Igor as waves. These waves were then saved as delimited text as a dat file into a matlab folder. The spectra were then loaded into Matlab along with the corresponding wavelength file. The program "Principle Component Analysis Function using the Singular Value Decomposition Function" was used on the data. The function was [var,cum_var,ut,st,vt,scores,evect,eval] = pca_svd(A,wv,k,flag); which corresponds to the following code:

```
if flag==1;

 [mc_A,avg] = mean_corr(A);
else
   mc_A=A;
end;
[u,s,v]=svd(A,0);
ut=u(:,1:k);
st=s(1:k,1:k);
vt=v(:,1:k);
if flag==1;
 [n,m]=size(A);
 means=ones(n,1)*avg;
 A=mc_A+means;
```

```
else
end;
eval=diag((s.^2));
evect=vt;
scores=A*evect; % calculation of the principal component scores
trace_of_A=sum(eval);
eval=eval(1:k);
var=100.0*eval/trace_of_A; % calculates percent variance
ssq=0;
resid_ssq=trace_of_A;
for i=1:k;
  ssq=ssq+eval(i,1);
  resid_ssq=resid_ssq-s(i);
        cum_var(i,1)=100.0*ssq/trace_of_A; end;
```

This function performs principal component analysis of a data matrix, 'A', it is trimmed to 'k' factors via the SVD function. The 'flag' indicates whether or not to perform mean correction (1 = mean correct the data set, 'A'). 'ut' is the matrix of trimmed column-mode eigenvectors, 'vt' is the matrix of trimmed row-mode eigenvectors, and 'st' is the square matrix of trimmed singular values. The vt(1-5), ut(1-5), time, and wavelength were then copied and pasted into Igor as waves. Graphs were then made of ut vs tt(time) and vt vs wl(wavelength). By determining the eigenvalue corresponding to the eigenvector, only the first two eigenvectors were used in each analysis.

A rotational matrix method was used to further separate out all the components of the reaction after performing the SVD. By rotating the eigenvector matrix, we were able to separate out the heme shift/degradation with the product growth and the substrate decrease. An example code using 45º is below:

```
r1=cos(45*PI/180)*v1+sin(45*PI/180)*v2
r2=-(-sin(45*PI/180)*v1+cos(45*PI/180)*v2)
t1=cos(45*PI/180)*17.6946*u1+sin(45*PI/180)*3.797*u2
```

```
t2=-(-sin(45*PI/180)*17.6946*u1+cos(45*PI/180)*3.797*u2)
```

This code replaces the eigenvectors with r1 and r2, and replaces the kinetics of the eigenvectors with t1 and t2 while multiplying them by some angle. The angle for the specific data is determined by trial and error until the original spectra is obtained by either r1 or r2. Some of the data was inverted by adding a minus sign in front of one of the equations as done above with r2 and t2. T1 and t2 have the eigenvalues included in their formulas, which were obtained from the Matlab file. Plots of r1, r2, v1, and v2 vs. wl(wavelength) were made to compare the data.

Non-Linear least squares fitting was performed on the kinetics plots(ut vs tt) and on the previous kinetics plots of specific wavelengths of the assay spectra. First order rate equations can be solved by performing an exponential fit dependent on the number of processes involved. Double exponential, tri-exponential, and quadratic exponential fits were used for all the kinetic data. Therefore, there are 1, 2, or 3 rate constants for each graph depending on the type of exponential fit used. Using an exponential fit for a first order rate equation can be proven by integrating the rate equation, which will result in an exponential function.

References:

[1] G. Sarkar and S.S. Sommer, The "megaprimer" method of site-directed mutagenesis. *Biotechniques*. **1990**, 8, 404-407.

[2] V. Mittal, DNA Array Technology. *Molecular Cloning: A Laboratory Manual* 3rd ed. Cold Spring Harbor Laboratory Press. **2000**, Appendix 10, Vol. 3.

[3] R. Varadarajan, A. Szabo, S.G. Boxer, Cloning, expression in Escherichia coli, and reconstitution of human myoglobin. *Proc. Natl. Acad. Sci.* U.S.A. **1985**, 82:5681-5684.

Chapter 3: Results and Discussion

3.1 Introduction

The contents of this chapter include the results of mutagenesis, purification, spectroscopy, and analysis. The enzymes, DHP, HRP, Y39F, H56R, and H90G and their reactions with different substrates [tribromophenol (TBP), trichlorophenol (TCP), and trifluorophenol (TFP)] were studied by a spectrophotometric assay and analyzed using kinetic fitting and singular value decomposition. The results of the spectroscopic assay reveal that the function of dehaloperoxidase does depend on both a proximal and distal histidine, H90 and H56, respectively. The results showed complete loss of activity for the mutants H56R and H90G. On the other hand, Y39F exhibited more activity than native DHP, but less than HRP. The rate constants for all the processes are reported and compared in this chapter. It was also learned that the heme was being degraded in all the mutants and native DHP for all the assays. The heme degradation was caused by hydrogen peroxide and was more apparent in DHP than in HRP. Singular Value Decomposition and a rotational matrix procedure was used to separate out the 3 or 4 components of the dehalogenating reaction of DHP. The final results revealed clues to a possible radical intermediate/polymerized product formation in DHP. As discussed in the introduction, radicals that are produced by one electron oxidation of phenol can escape the protein and initiate a polymerization. On the other hand, the more widely recognized two-electron oxidation leads to formation of a quinone. The spectroscopic assay provides an initial mechanistic hypothesis for a role for the one-electron oxidation in DHP.

3.2 Mutagenesis Results

3.2.1 Y39F Results

Mutagenesis was done on Y39F by PCR of three reaction mixes. The primary PCR product of Y39F is shown in the electrophoresis gel in figure 3.1. Different temperatures were used in the extension cycle. All of the temperatures used, 54°, 56°, and 58° C had positive results.

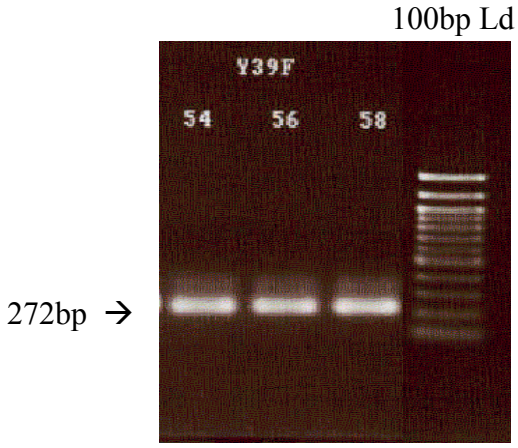

Figure 3.1 Y39F first PCR products made at 54°C, 56°C, and 58°C and 100bp ladder

The PCR fragment and the pET16b plasmid vector were digested with restriction enzymes. The restriction enzymes chosen to ligate the Y39F insert to the vector were at the 5' end, ncoI, and at the 3' end, sacI. A double digest was performed for the ligation of the fragments. The Y39F mutated insert and the vector were run on a gel and are shown in figure 3.2 to quantify the concentration of each. The ligation reaction depends on the ratio of vector to fragment.

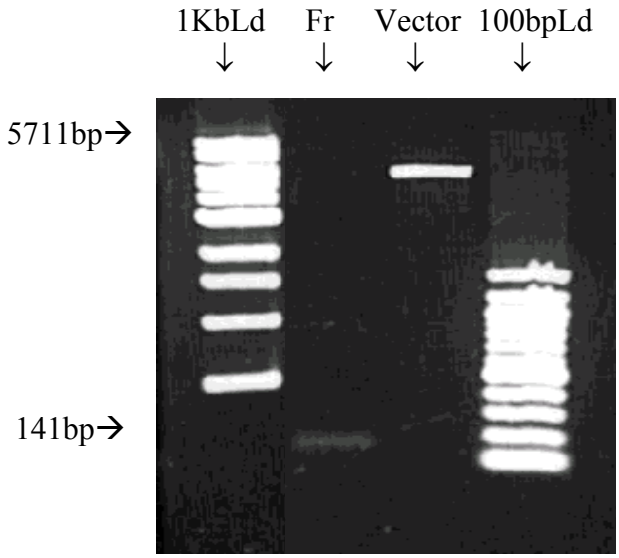

Figure 3.2 Y39F fragment and vector gel to compare concentrations. 1:5 ratio, fragment to vector

The ligation of the Y39F fragment to the vector was performed. After ligation, the DNA was transformed into *E. coli* cells on agarose plates with ampicillin and resulted in 6 colonies. The control plate, which contained DNA without the mutated fragment had 1 colony. The plasmid DNA was extracted and a test digest was performed on four transformants to confirm the mutation. Figure 3.3 confirms that transformants #2 and #4 were digested properly because there are 3 bands. The mutated restriction sites were cut with the enzymes resulting in three bands of different weights.

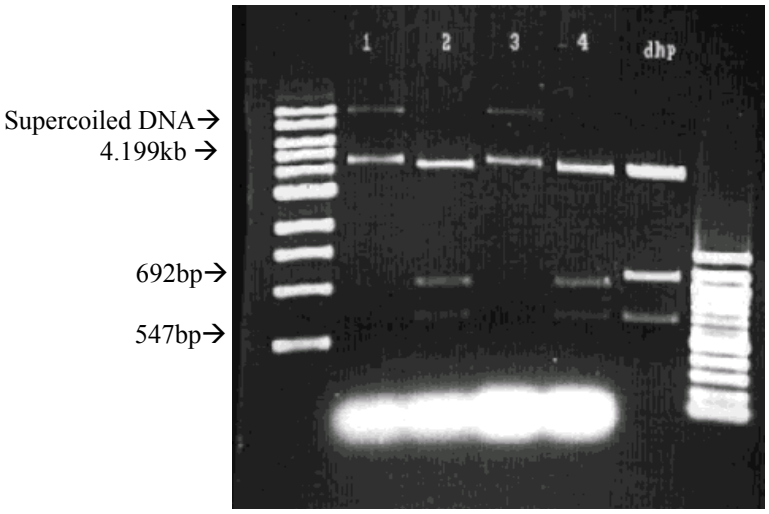

Figure 3.3 Gel for Y39F test digests 1-4 and DHP as the control. Digests #2 and #4 digested properly. The restriction enzyme used was draI.

After digests #2 and #4 were transformed into competent *E. coli* Rosetta® competent cells and plated on agarose plates with ampicillin, the results were positive. The cell growth on the Y39F#2 plate was 83 colonies. The cell growth on the Y39F#4 plate was 75 colonies. After the DNA was grown and a plasmid purification was performed on the cells, the DNA was sequenced. The T7 promoter primer was used to sequence the DNA. The results of the sequencing are shown in figure 3.4.

Y39F4

```
ATG GGG CAC CAC CAC CAC CAC CAC GGG TTT AAA CAA GAT ATT GCC ACC ATC CGC
GGT GAT CTC AGG ACC TAT GCA CAG GAC ATT TTC CTC GCA TTT TTG AAT AAG TAC
                          C           A
CCG GAC GAG AGG AGG TAC TTT AAA AAC TTT GTC GGC AAA TCT GAC CAA GAG CTC
AAG TCA ATG GCC AAG TTC GGT GAT CAC ACT GAG AAA GTG TTC AAC CTG ATG ATG
GAA GTT GCG GAC CGA GCC ACC GAT TGT GTC CCC CTT GCG TCC GAC GCC AAC ACA
CTC GTC CAG ATG AAA CAG CAT TCC AGC CTG ACG ACT GGA AAC TTC GAG AAA CTG
TTC GTG GCA TTG GTG GAG TAT ATG AGA GCG TCT GGC CAG TCC TTC GAC TCT CAA
AAG CTG GGA TAG GTT CGG CAA GAA TTT GGT CTC CGC GCT GAG CAG CGC AGG CAT
GAA GTAG
```

Figure 3.4 The Y39F sequence. The mutated nucleotides are in highlighted and the native nucleotide above it is highlighted.

After sequencing the DNA, it was transformed into *E. coli* cells and the cell pellets with the expressed protein was stored at -20°C. The pellets were light red and turned redder over time (observed for a period of days).

3.2.2 H56R and H90G Mutagenesis Results

After the mutations were made and the dpnI enzyme was added to the reaction mixes, the DNA was transformed into competent *E. coli* cells. The transformations were numbered for future references. The results of the transformation into the competent *E. coli* cells for the H90G#2 reaction had 13 colonies and H90G#1 reaction had one colony. The results of the H56R#4 *E. coli* cell transformation reaction was 1 colony, H56R#5 had 7 colonies, and H56R#6 had 3 colonies. Figure 3.5 shows the gel for the restriction digest of H90G with xhoI. The restriction enzyme cut the vector and linearized it making

a 6065bp fragment. The uncut bands show two peaks, one that is supercoiled DNA and the other is plasmid DNA.

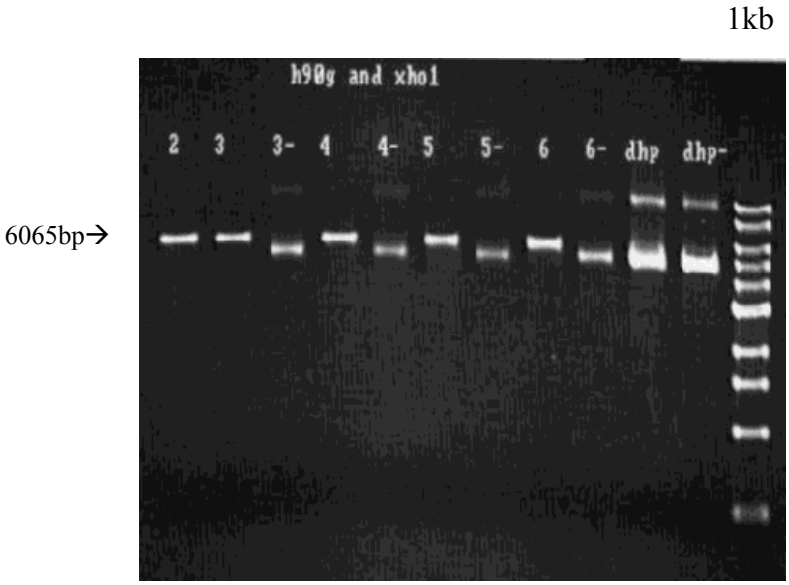

Figure 3.5 Gel for digestion of H90G with xhoI. Uncut bands have a – after the number. Digests 3-6 cut properly.

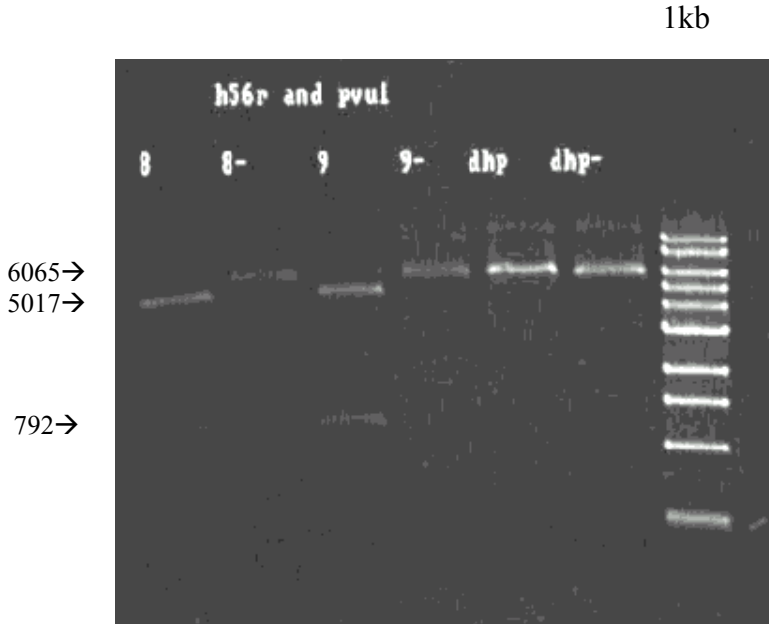

Figure 3.6 Gel for digestion of H56R with pvuI. Uncut bands have a – after the number. Digests 8 and 9 are shown and were used.

Figure 3.6 shows gel for the restriction digest for H56R with pvu1 to determine whether the mutation was made or not. The gel shows that the cut plasmid has two bands of the right size, and the uncut has a band at 6065bp. After the DNA was cleaned with a plasmid purification kit, it was sequenced. The PETUP primer was used for sequencing both mutants. The results of H56R and H90G sequencing are shown in figure 3.7 and figure 3.8.

H56R8

```
ATG GGG CAC CAC CAC CAC CAC CAC GGG TTT AAA CAA GAT ATT GCC ACC ATC CGC
GGT GAT CTC AGG ACC TAT GCA CAG GAC ATT TTC CTC GCA TTT TTG AAT AAG TAC
CCG GAC GAG AGG AGG TAC TTC AAA AAC TAT GTC GGC AAA TCT GAC CAA GAG CTC
                          T       A
AAG TCA ATG GCC AAG TTC GGC GAT CGC ACT GAG AAA GTG TTC AAC CTG ATG ATG
GAA GTT GCG GAC CGA GCC ACC GAT TGT GTC CCC CTT GCG TCC GAC GCC AAC ACA
CTC GTC CAG ATG AAA CAG CAT TCC AGC CTG ACG ACT GGA AAC TTC GAG AAA CTG
TTC GTG GCA TTG GTG GAG TAT ATG AGA GCG TCT GGC CAG TCC TTC GAC TCT CAA
AGC TGG GAT AGG TTC GGC AAG AAT TTG GTC TCC GCG CTG AGC AGC GCA GGC ATG
AAG TAG
```

Figure 3.7 Nucleotide sequence of H56R #8. The mutated nucleotides are highlighted and above them are the native nucleotides highlighted.

H90G5

ATG GGG CAC CAC CAC CAC CAC CAC GGG TTT AAA CAA GAT ATT GCC ACC ATC CGC

GGT GAT CTC AGG ACC TAT GCA CAG GAC ATT TTC CTC GCA TTT TTG AAT AAG TAC

CCG GAC GAG AGG AGG TAC TTC AAA AAC TAT GTC GGC AAA TCT GAC CAA GAG CTC

AAG TCA ATG GCC AAG TTC GGT GAT CAC ACT GAG AAA GTG TTC AAC CTG ATG ATG

GAA GTT GCG GAC CGA GCC ACC GAT TGT GTC CCC CTT GCG TCC GAC GCC AAC ACA

CAT C

CTC GTC CAG ATG AAA CAG **GGC** TC**G** AGC CTG ACG ACT GGA AAC TTC TAG AAA CTG

TTC GTG GCA TTG GTG GAG TAT ATG AGA GCG TCT GGC CAG TCC TTC GAC TCT CAA

AGC TGG GAT AGG TTC GGC AAG AAT TTG GTC TCC GCG CTG AGC AGC GCA GGC ATG

AAG TAG

Figure 3.8 The nucleotide sequence for H90G#5. The mutated nucleotides are highlighted and above them are the native nucleotides highlighted.

3.3 Spectroscopic Assay Results

Spectroscopic probing of the reaction was done to understand the appearance of product and the disappearance of substrate. In addition, the Soret band, which contains information about the heme active site, was monitored. This assay is based on the knowledge that peroxide will bind to the enzyme and allow the enzyme to bind the trihalophenol substrate. The assays were run at 20°C in a quartz cuvette with a UV-vis spectrometer and kinetic assays were run taking a spectrum every 3 seconds. In the following figures of the kinetics, around 30 spectra were exported to exemplify the total time course reaction.

The Soret band is observed in all of the time-dependence spectra. The wavelength of the Soret band ranges from 409nm to 421nm depending on the coordination and spin state of the heme iron. The final enzyme concentration in the reaction was determined by using the known CO bound DHP or compound II form extinction coefficient, which is 188,000$M^{-1}cm^{-1}$ (Stefan Franzen et. al.). The ferric DHP extinction coefficient is about 150,000 $M^{-1}cm^{-1}$ and the oxyferrous DHP coefficient is about 164,000 $M^{-1}cm^{-1}$. The maximum of the Soret band shifts with oxidation and ligation of the heme iron. For DHP, 409 nm is the ferric form and 421 nm is compound II in the spectra reported below. It was found that the mutants, H56R and H90G, were in the oxyferrous form in the reactions, which is found at 414nm. In separate control experiments performed by Jennifer Belyea et. al. on DHP, it was found that the oxyferrous and the ferric forms of DHP gave the same results.[1]

The spectra contain a substrate peak, which decreases as time increases. The substrate peaks absorb at different wavelengths depending on the substrate.

Tribromophenol is shown at 315nm or 317nm and is decreasing over time. The product is increasing over time and is shown at 290nm or 294nm depending on the enzyme. In H90G and H56R the product peak is either non-existent or it is very small depending on the substrate, whereas Y39F shows a faster product growth than DHP.

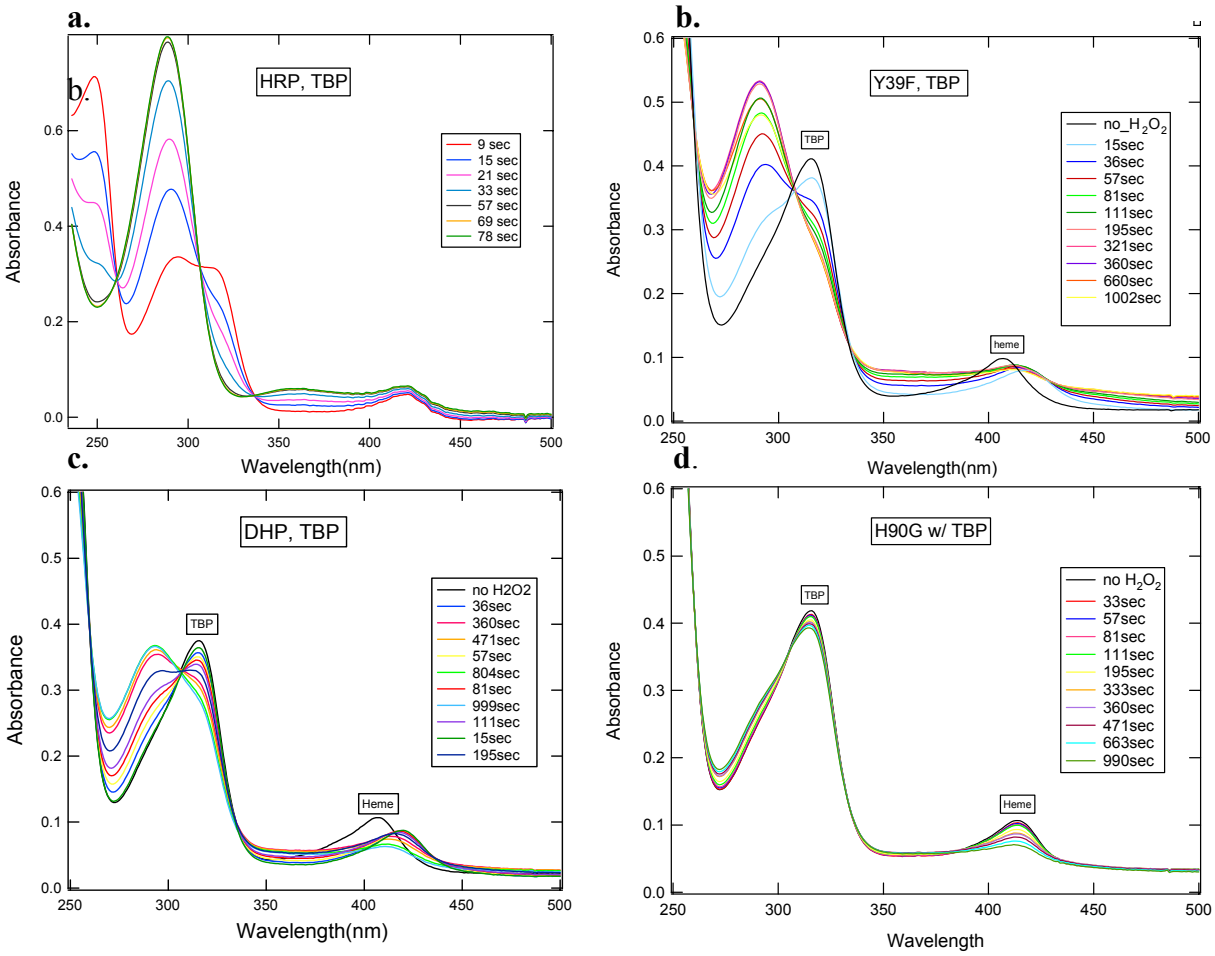

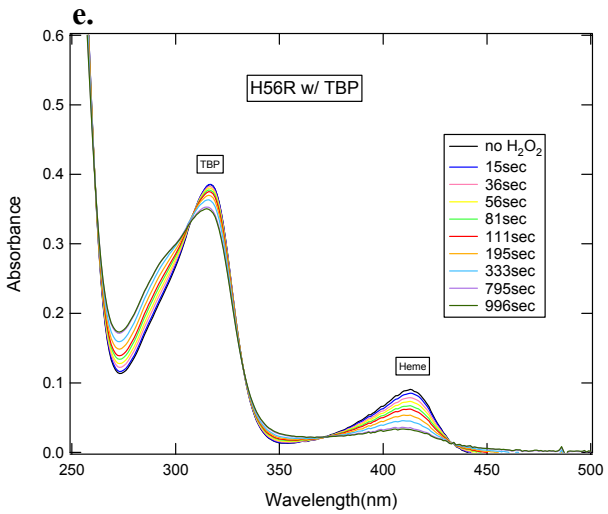

Figure 3.9 UV-Vis Spectra over time for all enzymes with Tribromophenol. Each color corresponds to a different length of time the reaction has processed. a. HRP b. Y39F c. DHP d. H90G e. H56R

Figure 3.9 shows kinetic assays for each enzyme with tribromophenol as a substrate. The general features observed here are also observed in the other substrates. H56R and H90G show little to no activity, whereas, Y39F shows more activity than DHP. Figure 3.9 shows that the heme is being degraded in the mutants and in DHP. This is observed by the decrease in intensity of the Soret band with time. The Soret band in HRP shows much less heme degradation. The spectra also show a shift in the Soret peak, which is labeled Heme on the plots, for all the enzymes except H90G and H56R. The conclusion at this point is that the heme shift is related to the product growth because the mutants that had little product growth had no Soret band shift.

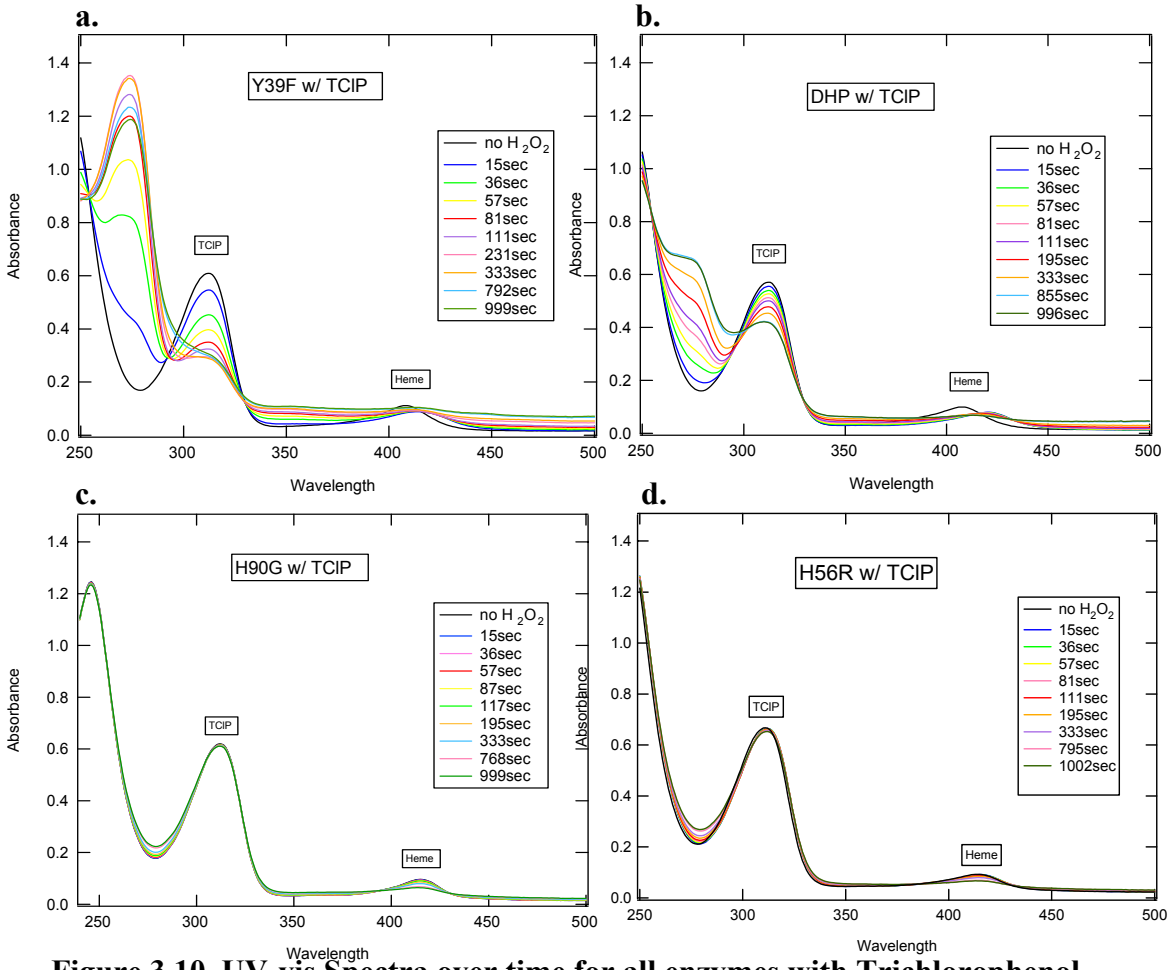

Figure 3.10 UV-vis Spectra over time for all enzymes with Trichlorophenol. Each color corresponds to a different length of time the reaction has processed. a. Y39F b. DHP c. H90G d. H56R

Figure 3.10 shows the results of the assay with trichlorophenol as the substrate. The conditions were the same for the TCP assay as they are for the TBP assay. The TCP peak is found at around 312nm and the product peak is found around 274nm. The Soret band shifts in the TCP assay as well. Figure 3.11 shows the same assay as the previous but the TCP concentration has been decreased by ½.

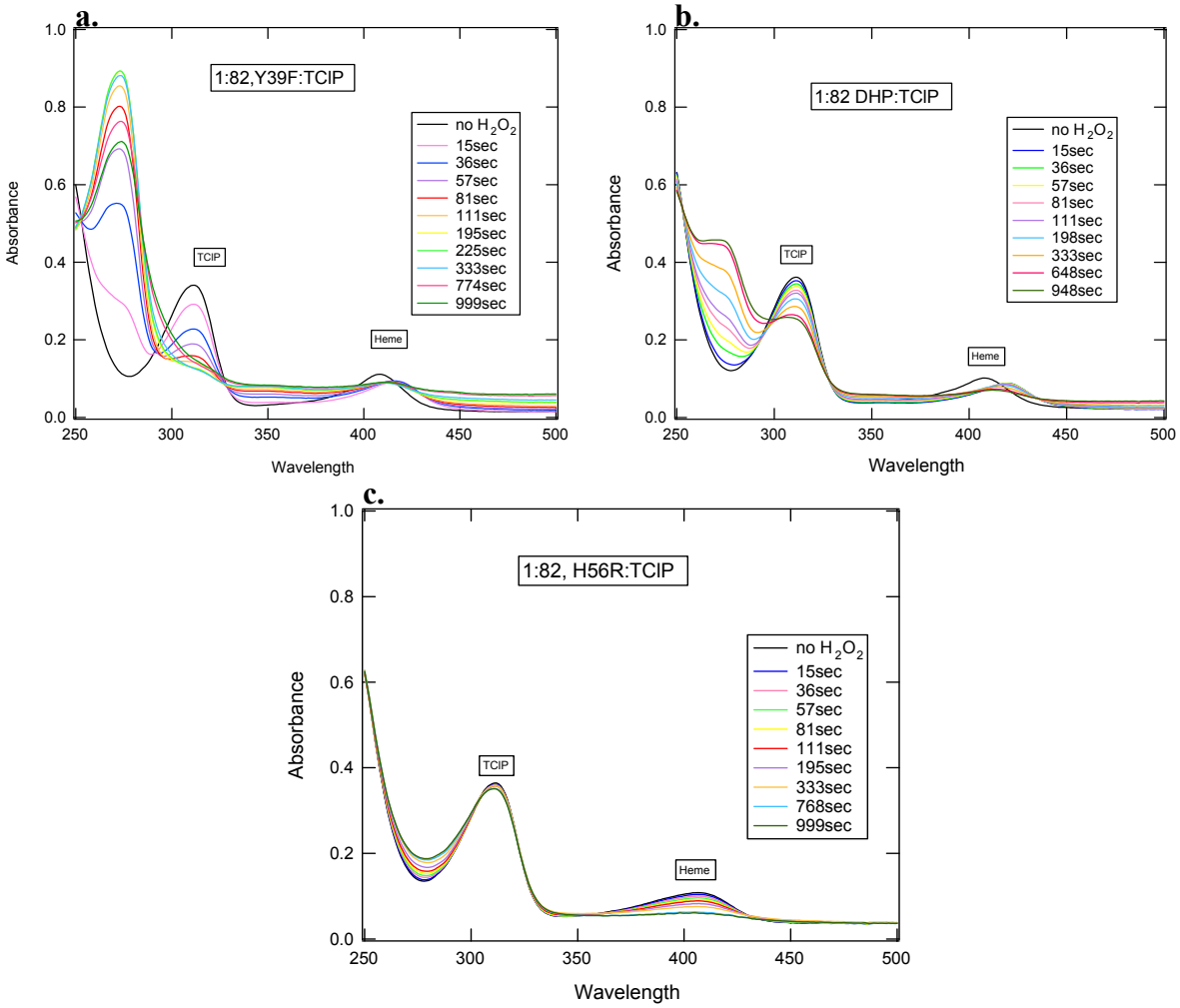

Figure 3.11 UV-Vis Spectra over time for all enzymes with Trichlorophenol (Enzyme:Substrate, 1:82). Each color corresponds to a different length of time the reaction has processed. a. Y39F b. DHP c. H56R

The results of the TCP assay where the concentration of TCP was decreased by half had an enzyme:substrate concentration ratio of 1:82, whereas, the previous TCP assay had a ratio of 1:164. These two ratios were compared to understand if the substrate was causing the heme degradation and to understand if the product increase would be affected by the decrease in substrate. It does appear that the product concentration is affected by the concentration of the substrate. A comparison of the amount of product and the extent of heme degradation was done. A series of experiments were carried out at constant

peroxide concentration, but with two different concentrations of TCP. The heme degradation does not seem to be affected by the concentration of the TCP, but further analysis will help to confirm this hypothesis. There possibly could be a competition between reaction with substrate and heme degradation, which could be more complicated. If the peroxide is not being used for substrate turnover, then it is possible that it degrades the heme. DHP rate constant for heme degradation is 0.0068 for the peroxide only assay. The rate constants for the DHP TCP assay for heme degradation are 5.341e-05, 0.00589, 0.00293. By comparing the rate constants for heme degradation for the peroxide assay and the TCP assay, it seems that there is faster heme degradation in the peroxide only assay.

Figure 3.12 shows the kinetics of the assay with trifluorophenol for three of the enzymes. The trifluorophenol assays show a large baseline change over time and this makes it difficult to decipher whether the heme is degrading over time. just by looking at the kinetic data. Some general trends still apply even in this assay. The product peak grows in at 345nm and the substrate peak decrease at 260nm. DHP and Y39F show more activity than H56R which has no activity except for heme degradation. It is observed that in the figure 3.12 c where there is no product increase and therefore, no scattering, that the heme is still being degraded.

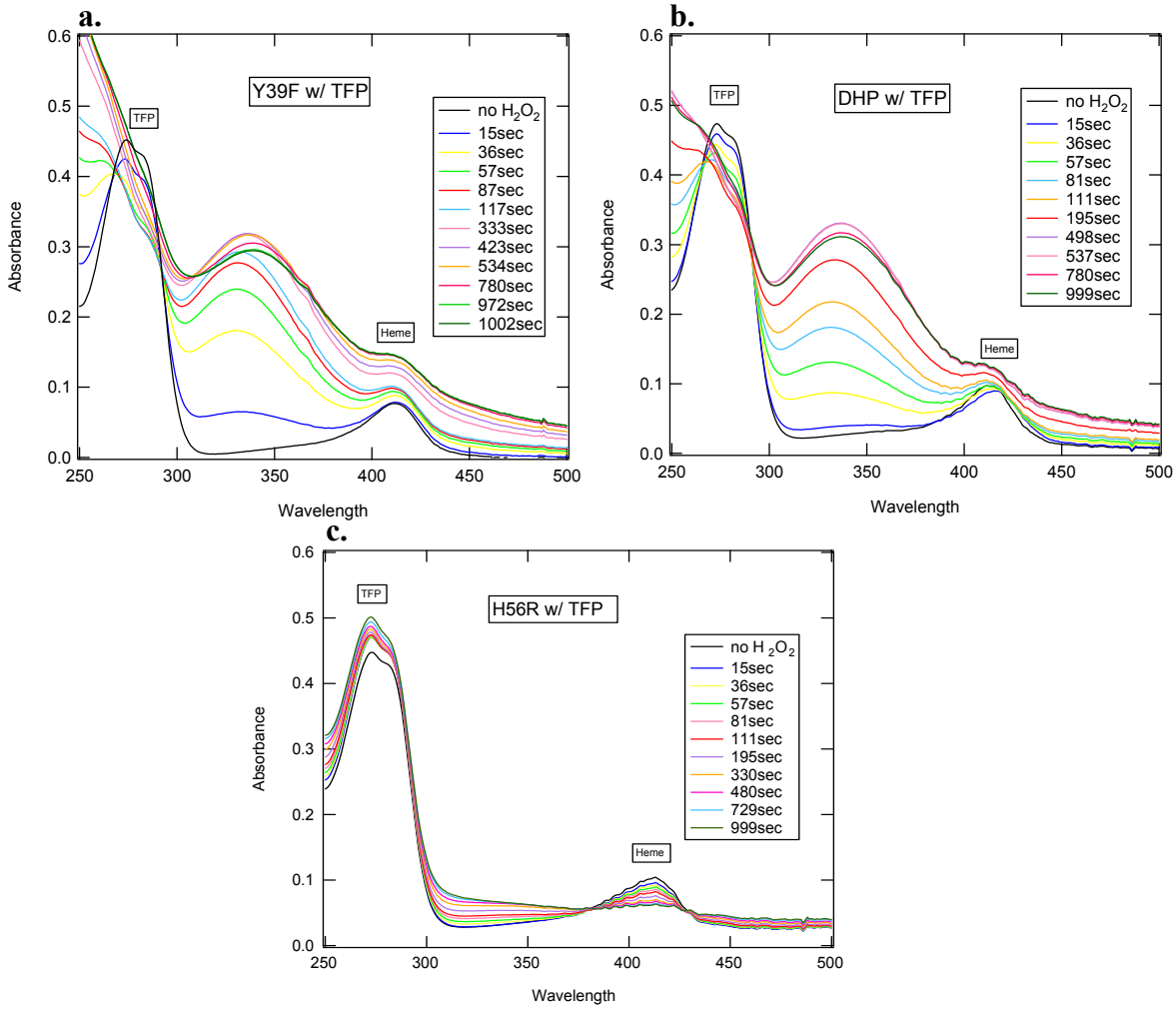

Figure 3.12 UV-Vis Spectra over time for all enzymes with trifluorophenol. Each color corresponds to a different length of time the reaction has processed. a. Y39F b. DHP c. H56R

Because time course is difficult to judge just by looking at the UV spectra, some kinetic graphs have been made of specific wavelengths of interest. These graphs were fit to exponentials in order to determine the rate constants associated with them. The rate constants of the different enzymes can be compared.

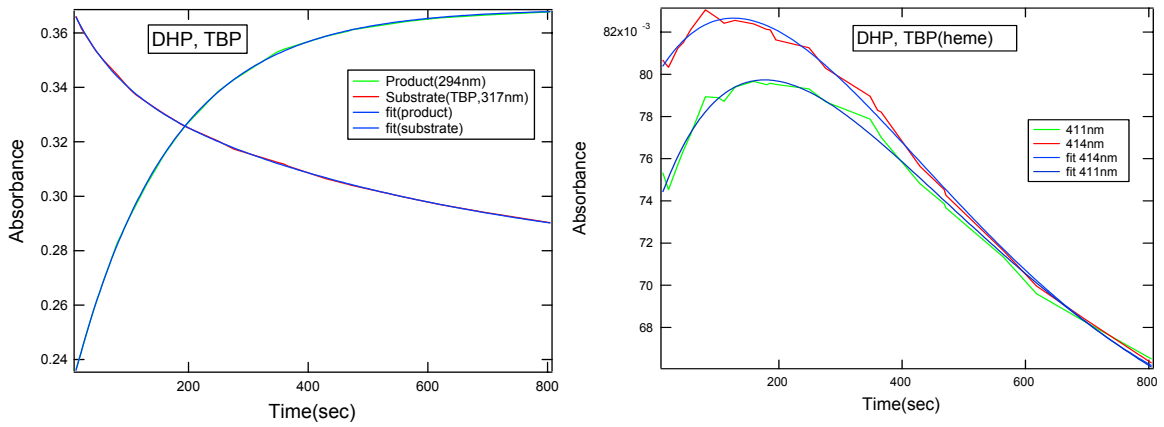

Figure 3.13 Kinetic spectra of particular wavelengths of interest with fitted lines of the DHP TBP reaction. The product, substrate, and heme peaks are represented here.

Table 3.1 shows the rate constants for the TBP and peroxide-only data associated with three wavelengths (414nm, 317nm, 290nm). The rate constants were found by performing non-linear least squares fitting by one, two, three, or four exponentials on the peak. The heme peaks are different by a few nanometers in the mutants and DHP.

Further analysis of the assays is needed for several reasons including differences among the mutants, DHP, and HRP. The rate constants for the heme peak are not comparable because Y39F and HRP are increasing, while the rest are decreasing. The Soret peak that corresponds to compound II increases and shifts to 421nm at the same time. The heme peak for the DHP TBP assay also has a slight increase at the start of the assay as shown in figure 3.13.

The substrate consumption and product growth rate constants for HRP TBP are very close to 1:1, but for the other enzymes they are all different. While some rate plots have a slow component and a fast component, others just have one or the other. Because the heme is being degraded in all but the HRP assays, the specific mechanism cannot be decided from these data alone. DHP must have a different mechanism than HRP which may not involve peroxide as the cosubstrate. The fact that substrate consumption and

heme degradation occur with the same rate constant indicates that peroxide will attack the heme as readily as substrate. This observation is difficult to reconcile with a mechanism that requires a peroxide cofactor *in vivo*.

Rate Constants from the Original Assay

	Heme (414nm)		Substrate(317nm)		Product (290nm)	
	ΔA	k	ΔA	k	ΔA	k
HRP TBP	**-0.031**	**0.045**	**0.385**	**0.062**	**-0.857**	**0.065**
HRP H_2O_2	**0.015** **-0.032** **0.034**	**0.002**[a] **0.036** **0.000**	---------	----------	----------	----------
Y39F TBP	**-0.0187** **-0.0157** **0.1068**	**0.0030** **0.0367** **0.00053**	**0.0748** **0.0650**	**0.016**[b] **0.044**	**-0.252** **-0.0921**	**0.020** **0.055**
Y39F H_2O_2	**0.0135** **0.0622**	**0.0264** **0.0015**	---------	----------	----------	----------
DHP TBP	**0.138** **-0.076** **0.0177**	**0.0035** **0.0017** **0.000**	**0.0726** **0.0272**	**0.002** **0.014**	**-0.143**	**0.006**[c]
DHP H_2O_2	**0.0297**	**0.0068**	---------	----------	----------	----------
H56R TBP	**0.118** **-0.0279** **0.0223**	**0.001** **0.003** **0.000**	**0.0159** **0.1053**	**0.003**[b] **0.001**	**0.163** **-0.0801** **0.213**	**0.001** **0.003** **0.000**
H90G TBP	**0.0461**	**0.00155**	**-0.0021** **0.0156** **0.402**	**0.002**[b] **0.005** **2.3e-5**	**-0.0175** **-0.0143**	**0.0037** **0.0031**
H90G H_2O_2	**0.0565**	**0.00249**	---------	----------	----------	----------

Table 3.1 Rate constants for the component wavelengths from the original assay. The label "enzyme H_2O_2" means there is no substrate in that assay. Where some assays have more than one rate constant, this implies it was fit by a double exponential or triexponential. a. 419nm b. 315nm c. 294nm

ΔA in table 3.1 represents the change in absorbance for the plot correlated to the rate constant. If there are 3 rate constants, then there are 3 ΔA's.

3.4 SVD Analysis Results

The issues concerning differences in wavelengths among the enzymes and separating out the many components of the reaction, and discussed previously will be elucidated by SVD (Singular Value Decomposition). The data were modified to optimize the SVD analysis. The spectra were truncated to include one substrate peak, the product peak, and the Soret band. The SVD matrix was then rotated at different angles to obtain separate components. Each substrate assay was rotated and kinetics plots were made of the rates that correspond to the eigenvectors and these are shown in the Figures 3.14 through 3.23. In each section following, the SVD results of the four substrate assays and a peroxide-only assay are shown.

3.4.1 Tribromophenol Assay

Tribromophenol (TBP) is known to be a natural pollutant near *Amphitrite ornata* on the ocean floor produced by *Notomastus lobatus* and other marine organisms.[2] Because of this, the substrate focused on most in this thesis is TBP. After SVD analysis of the reaction, the basis spectra were plotted and rotated to give Figure 3.14. Each enzyme in this study is analyzed in this figure. R1 and r2 in these figures are the red lines and represent the rotated eigenvector matrices. V1 and v2 are the blue lines and represent the eigenvectors from SVD analysis. They are plotted on the same graph to as an illustration of the effect of SVD matrix rotation. All of the basis spectra were rotated at different angles. It is important to note that in the rotated data, the basis spectrum r1 contains the heme and substrate peaks with no product bands. R2 has the appearance of a difference spectrum, in which the positive bands are the product bands and the negative bands correspond to substrate. R2 also contains a negative Soret band. R2dif represents

r1 + r2 and represents the product band. R2dif contains a small heme peak shift in Figs.3.14.b and c. Figure 3.1.4.a shows a heme peak for r1 at 421nm and r2 does not have a λ max peak, but r2dif shows a peak at 421nm. The HRP TBP analysis spectra showing only a heme peak at 421nm corresponds to the well-known spectrum of Compound II. The heme peaks in figure 3.1.4.c. for r1 show a λ max at 421nm and r2 shows a λ max at 423nm. The heme peaks in figure 3.1.4.b. show a max at 418nm for r1 and shows a negative λ max at 423nm. Y39F and DHP show inconsistent heme peak λ max for this assay which implies they all have their own mechanism which differs from HRP.

The peaks represented in certain spectra are related to one another. For instance, in r1 the two peaks are changing at the same time. R2 peaks change on a different time scale than the r1 peaks, which is why they were separated by rotational SVD. To analyze how fast the peaks are changing, plots of the kinetics were made and rate constants were found by non-linear least squares fitting.

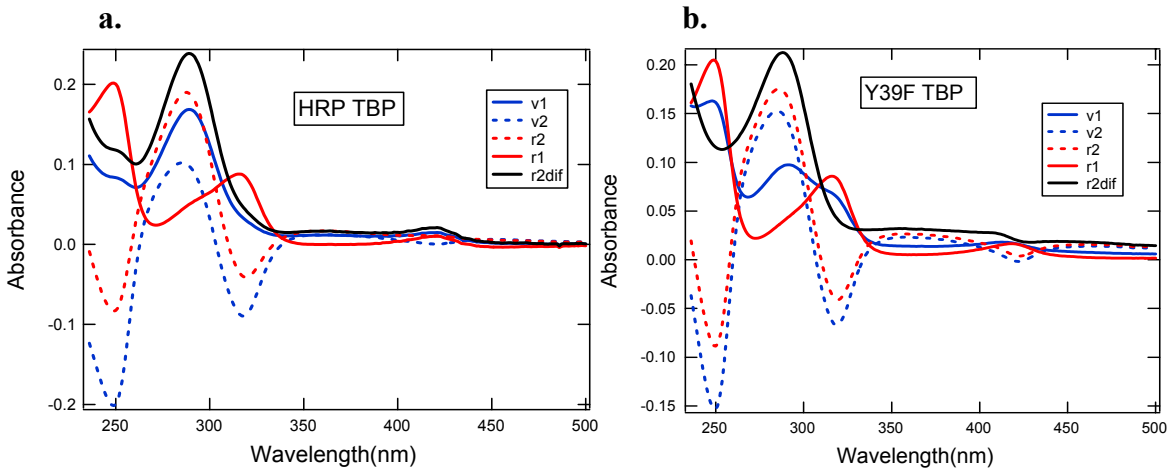

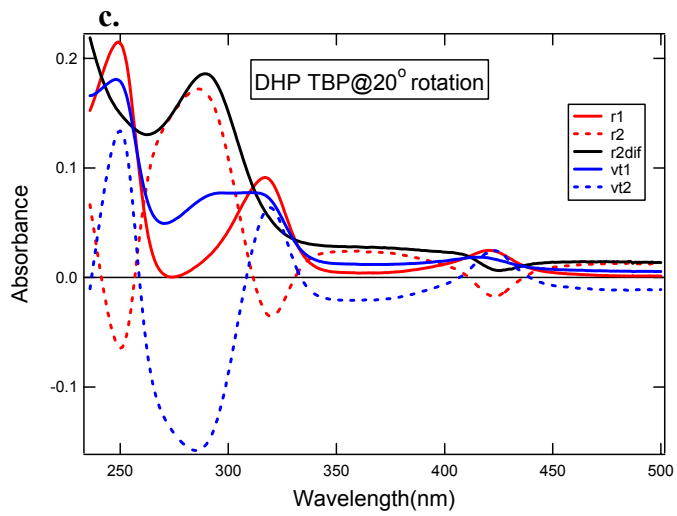

Figure 3.14 SVD Matrix Rotation for all the enzymes and TBP. a. HRP b. Y39F c. DHP

In figure 3.15 each rotated rate corresponding to the rotated basis spectra are plotted and fitted to one, two, three, or four exponentials to produce rate constants. SVD produces time courses that correspond to the basis spectra and figure 3.15 shows the rotated rates titled t1 and t2. T1 corresponds to the rate of r1 and t2 to r2. Because there are several peaks in r1 and r2, t1 and t2 contain several rates that will be discussed later. In figure 3.15 the plots are shown.

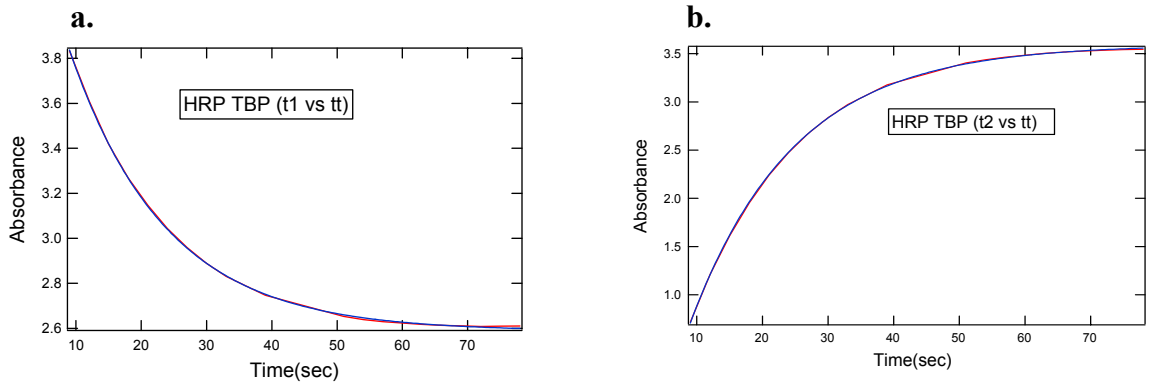

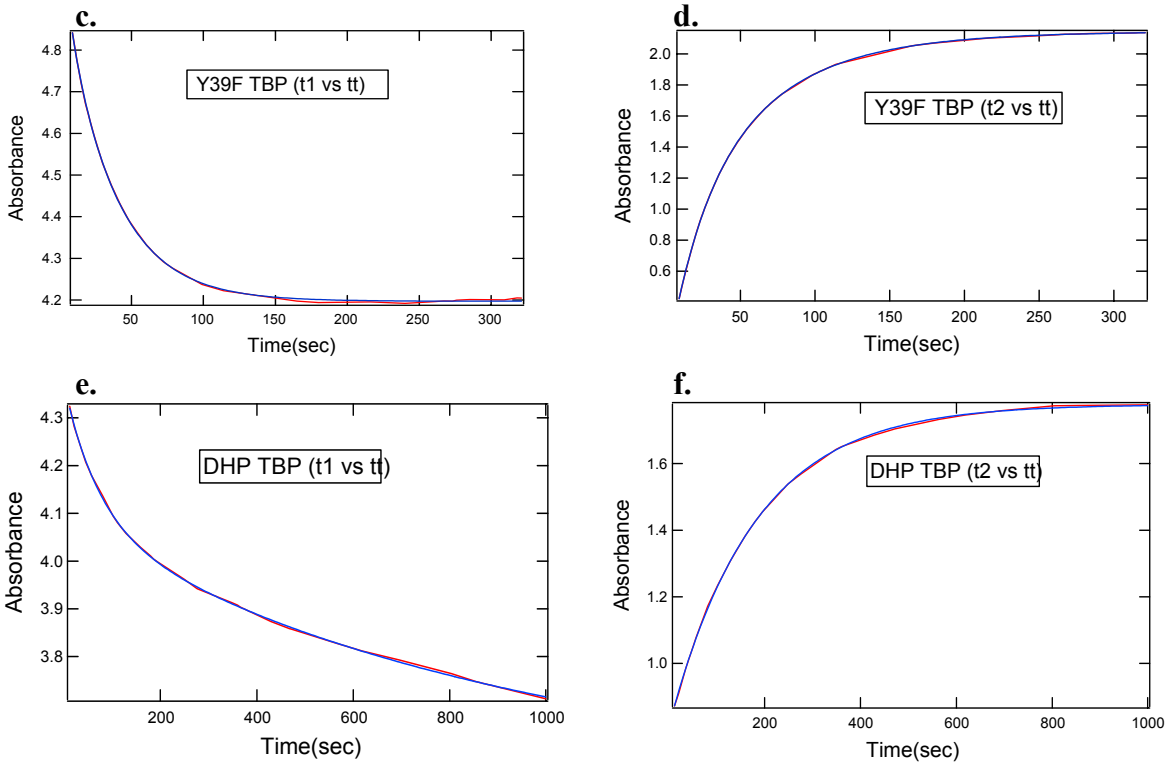

Figure 3.15 SVD Matrix Rotation Kinetics for all the enzymes with TBP. a. HRP t1 b. HRP t2 c. Y39F t1 d.Y39F t2 e. DHP t1 f. DHP t2

T1 for all the enzymes decrease at different rates, and t2 increases at different rates telling us that t2 contains product increase and t1 contains substrate and heme decrease. The results shown in figure 3.15. a.,b.,c., and d. illustrate that t2 increases faster than e. and f. which agrees with the previous assumption that Y39F and HRP have the fastest product growth when compared to the other mutants and DHP. The decay t1 and rise t2 are about equal in HRP. This is not the case for DHP or Y39F. In DHP, there is a biphasic decay with a fast component (comprising roughly half the amplitude). The rate constants indicate that substrate consumption is nearly twice as rapid as product growth at early times for DHP. In DHP, this could mean that the product is a dimer which is produced from two phenols (substrate). It is not known what the product of the DHP dehalogenating reaction is, but it is proposed that it contains a different composition

of products than HRP. The HRP assays seem to have direct turnover of substrate to product, whereas, the DHP and Y39F assays have properties that indicate a different mechanism and product.

3.4.2 Trichlorophenol Assay

To complete the analysis of DHP and its mutants, other substrates were used at the same concentrations including trichlorophenol (TCP). TCP is known to be another harmful pollutant that is now known to be dehalogenated by DHP and Y39F. The TCP analysis shows the same picture as the TBP analysis. In the DHP TCP plot, once again, r2dif has the characteristic heme shift as in the DHP TBP r2dif plot. The DHP TCP plot of r2dif also contains a slightly larger r2dif spectrum than in DHP TBP. Figure 3.16 b. shows a heme peak λ max at 421nm for r1 and a negative max at 422nm.

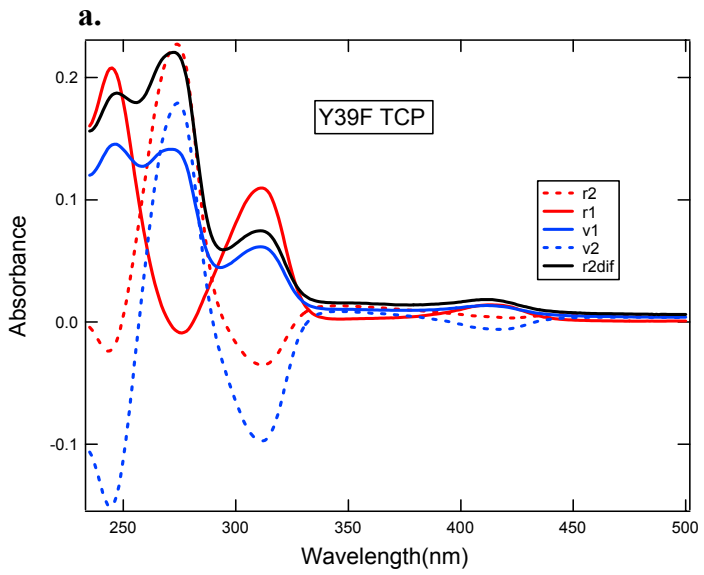

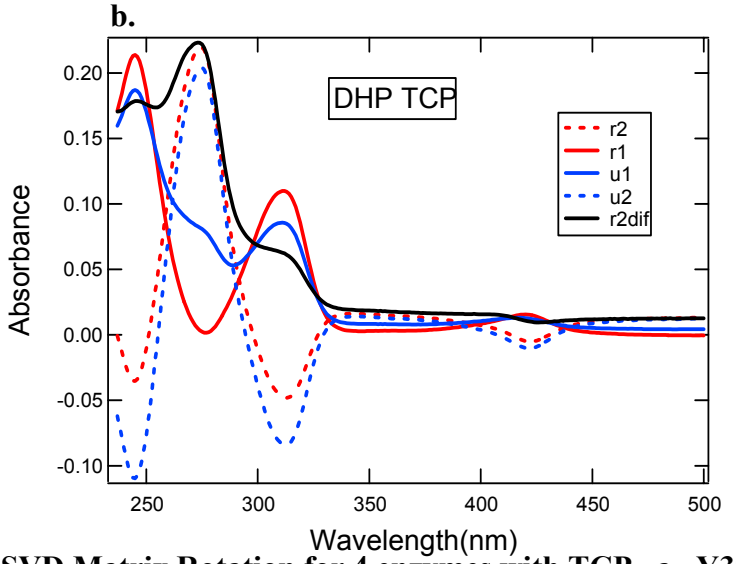

Figure 3.16 SVD Matrix Rotation for 4 enzymes with TCP. a. Y39F b. DHP

The rate plots of the TCP rotated data are shown in figure 3.16. The analysis of the TCP rate plots is slightly different than the TBP rate plots. Y39F and DHP show a decrease in t1. T2 is increasing in both of the enzymes, however substrate consumption is much more rapid in Y39F than DHP.

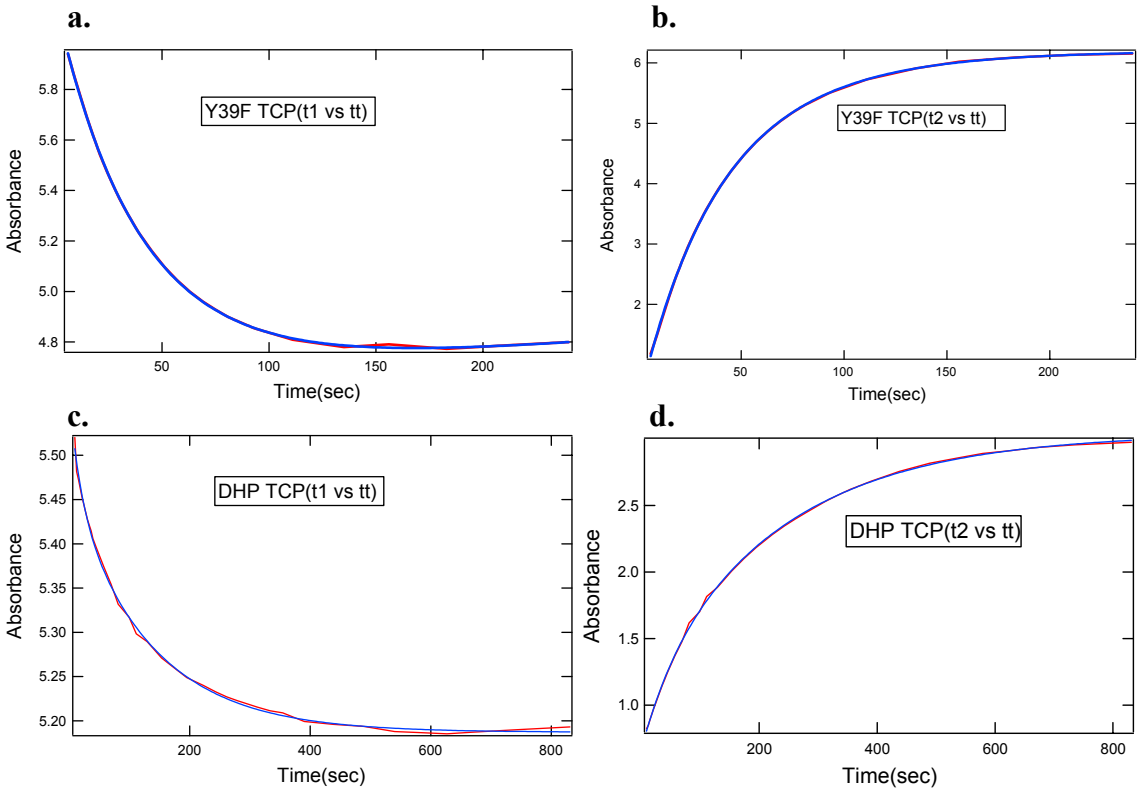

Figure 3.17 SVD Matrix Rotation Kinetics for the enzymes with TCP. a. Y39F t1 b. Y39F t2 c. DHP t1 d. DHP t2

3.4.3 49 μM Trichlorophenol Assay

To study whether the substrate or the peroxide is degrading the heme, an assay was performed with half the TCP concentration of the previous assays (49μM). If there are competing processes (oxidation of substrate and heme degradation) then the branching between these processes will depend on the substrate concentration. The SVD analysis in figure 3.18 shows the effect of decreasing the substrate concentration in half.

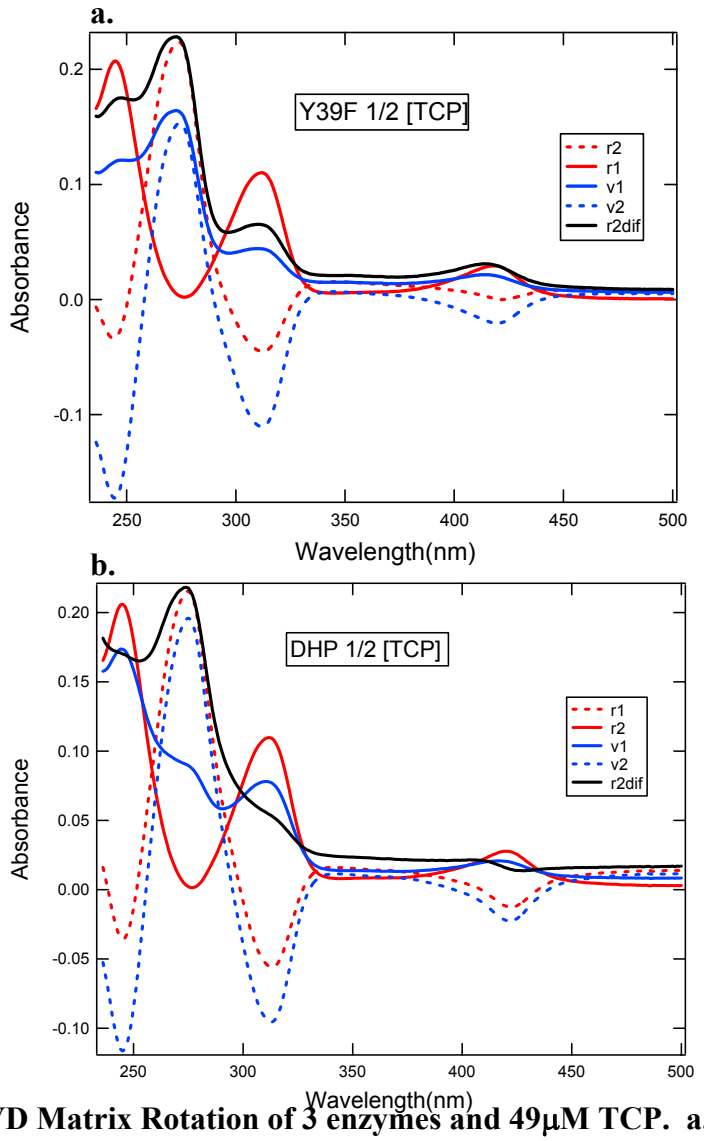

Figure 3.18 SVD Matrix Rotation of 3 enzymes and 49μM TCP. a. Y39F b. DHP

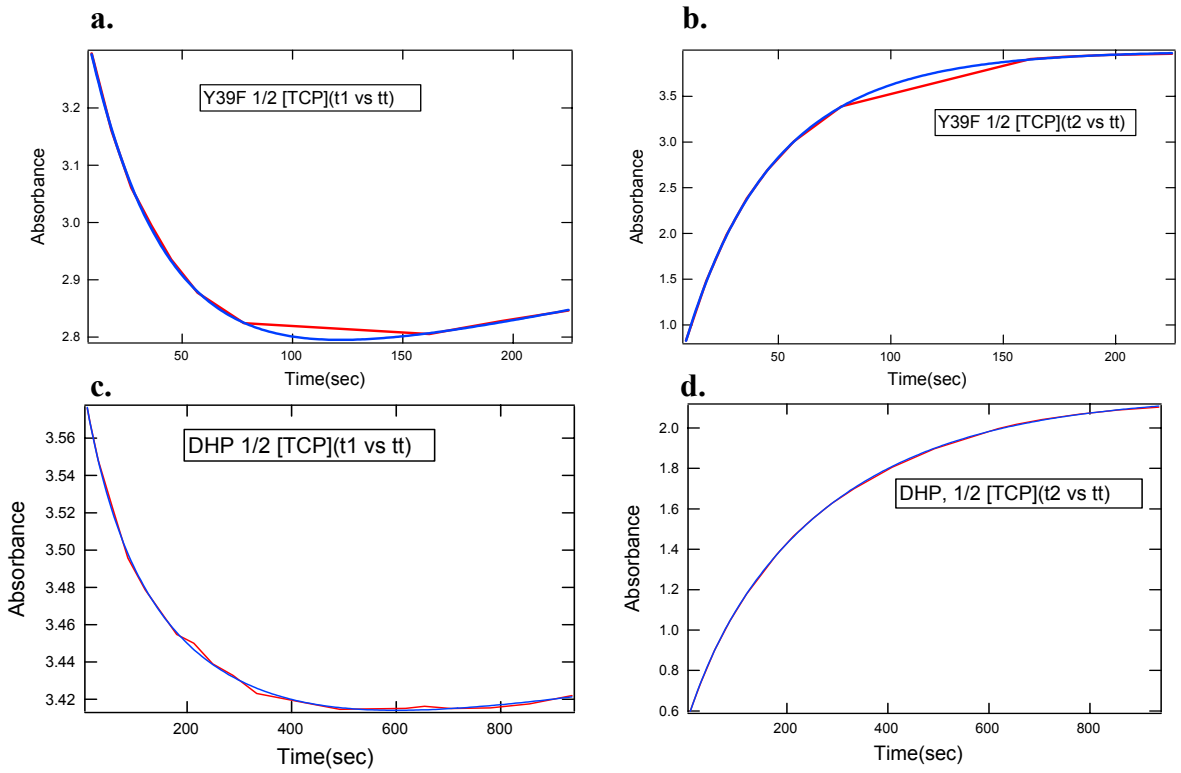

Figure 3.19 SVD Matrix Rotation Kinetics for 3 enzymes and 82μM TCP. a. Y39F t1 b. Y39F t2 c. DHP t1 d. DHP t2

The rate plots show that t2 (product growth) is increasing for both DHP and Y39F. Y39F is again faster than DHP in the 49μM TCP assay. But, the effects of decreasing the substrate by half also decreases the absorbance change for t2 in both DHP and Y39F. As one would expect, t1 decreases for Y39F and DHP. T1 decreases slower and t2 increases slower in the 82μM Y39F TCP assay than in the 49μM assay. However, DHP seems to have faster rate constants for t1 and t2 in the 82μM assay than in the 49μM assay. This indicates a differences in the mechanism and turnover rates between DHP and Y39F.

3.4.4 Trifluorophenol Assay

The reaction of DHP and H_2O_2 with trifluorophenol is of interest for two reasons. Firstly, the carbon fluorine bond is quite strong and it is rare to find an enzyme capable of oxidizing trifluorophenols. Secondly, TFP is much more soluble than TBP and has proven useful in some assay conditions. However, the trifluorophenol assays gave significantly different results from those for TCP and TBP. There appears to be an increase in the background of the absorption spectrum due to scattering as the product is formed in the TFP reaction catalyzed by DHP in the presence of H_2O_2. Figure 3.20 b. shows a DHP Soret band max for r1 at 419nm and a negative minimum for r2 at 421nm. Figure 3.20 a. shows a heme peak max for r1 at 412nm and a negative minimum at 417nm for r2. DHP and Y39F show a significant heme shift in the SVD data after matrix rotation, which is due to the formation of product.

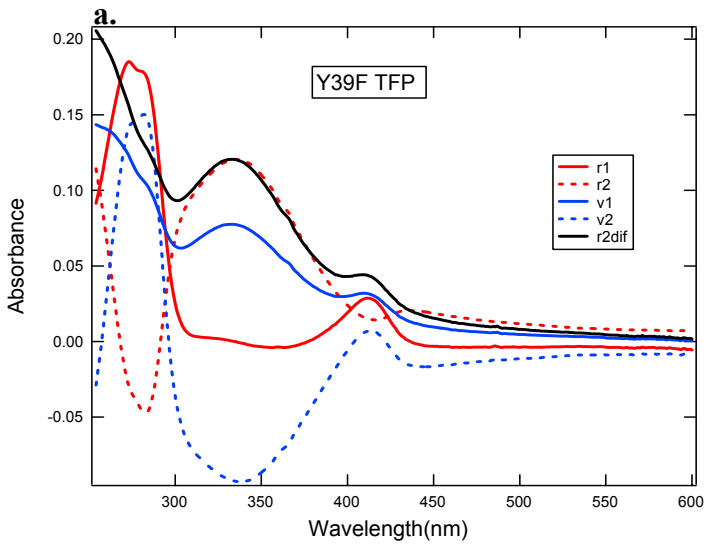

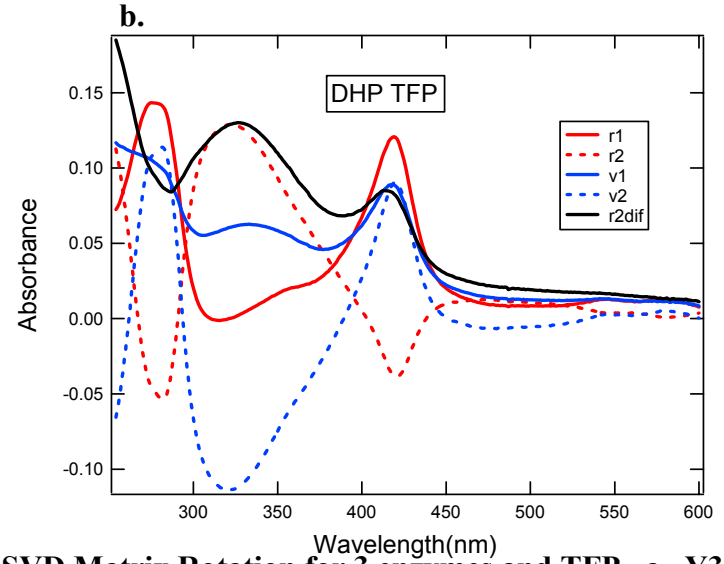

Figure 3.20 SVD Matrix Rotation for 3 enzymes and TFP. a. Y39F b. DHP

Previously it was shown that t1 decreased with the other substrates due to loss of heme and substrate, but the factors here are different and t1 increasing could be due to the overall change in the spectra. The baseline for the original kinetic assay for TFP increased as time went on and this should be considered when comparing the rate constants of the processes. Despite the baseline problem, t2 still shows the product increase to be more in Y39F than in DHP. The bottom line for the TFP assays is that DHP and Y39F degrade TFP and form a product, but Y39F forms product faster.

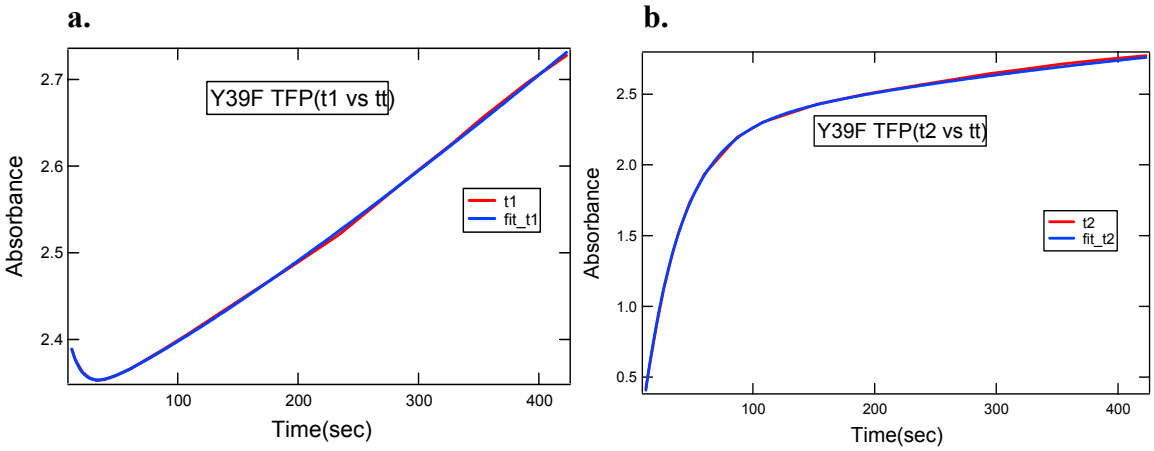

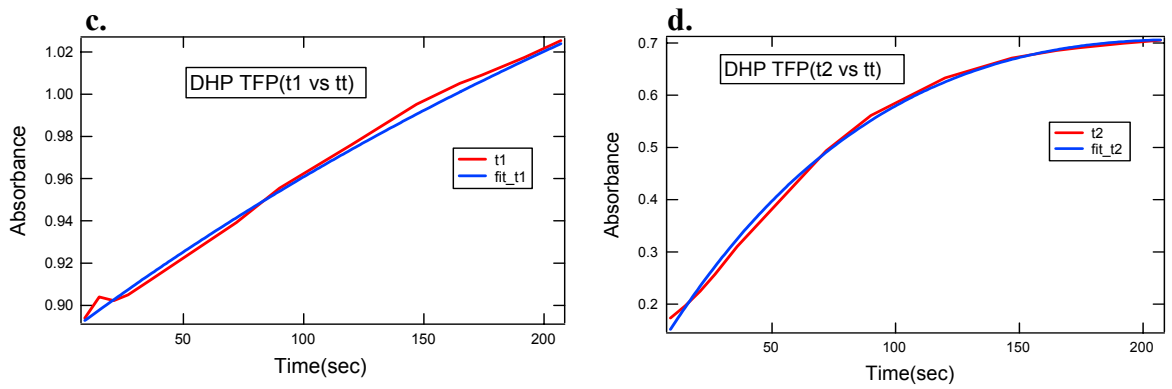

Figure 3.21 SVD Matrix Rotation kinetics for 3 enzymes and TFP. a. Y39F t1 b. Y39F t2 c. DHP t1 d. DHP t2

3.4.5 Hydrogen Peroxide Assay

To address the issue that the Soret band decreases over time in most of the assays, the assay with no substrate (peroxide only) has been analyzed by SVD. The important question of whether the heme peak in DHP degrades faster than HRP and if so how much faster, will be answered here. The other question that will be answered is, since Y39F has shown to have activity better than DHP but worse than HRP, will the heme degrade on the same order as its native enzyme or is it a function of activity that degrades the heme?

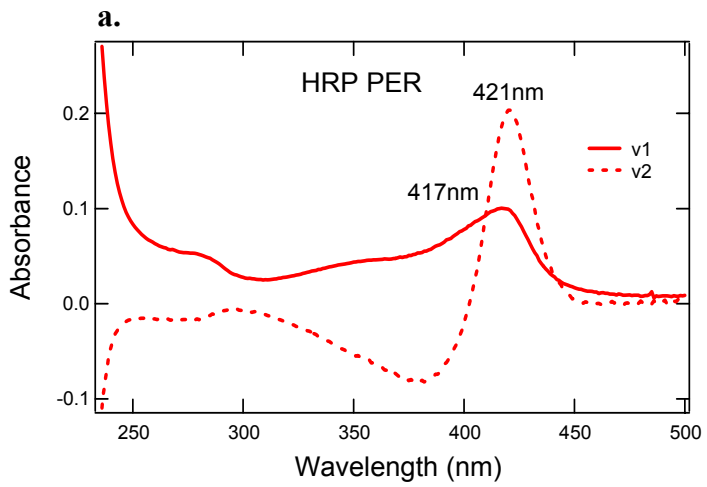

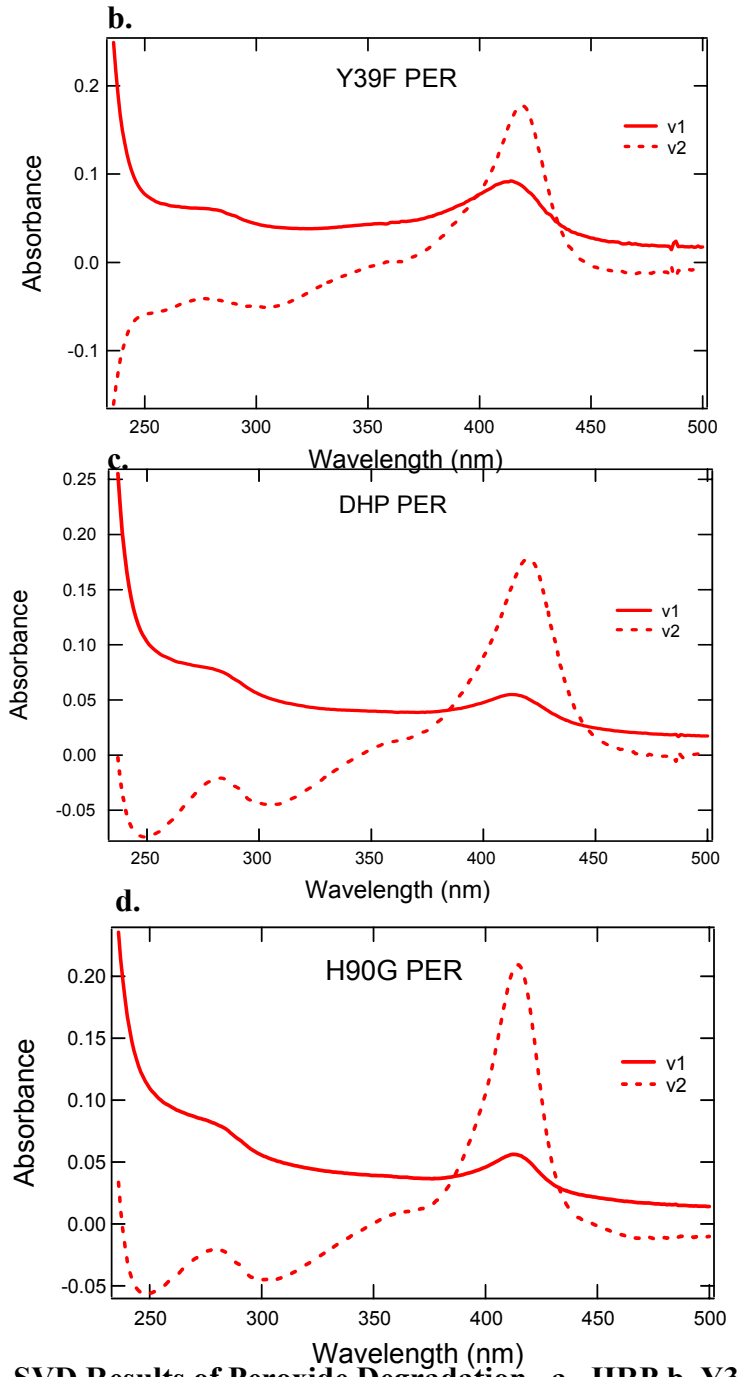

Figure 3.22 SVD Results of Peroxide Degradation. a. HRP b. Y39F c. DHP d. H90G

The rate plots are shown in figure 3.23 and show the rate of heme degradation or growth when compound II is formed without the substrate being present. In the case of HRP, it is likely that the intermediate compound I is also detected under these conditions.

Evidence for this can be seen in the v2 basis spectrum. The dip near 380nm may indicate a difference spectrum between compound II (positive lobe at 421nm) and compound I (negative lobe at 379nm). It is the case that HRP in figure 3.23 has a sharp positive slope in the beginning of the assay for both u1 and u2. This rapid process that is absent in DHP and the Y39F mutant is likely a kinetic feature due to the formation of compound II. T2 in HRP PER, however, shows a decrease as a function of time that may arise from heme degradation. Heme degradation is known in HRP and has been reported as the end product P670. Based on the HRP spectra we can interpret the DHP and Y39F spectra as indicating that compound II is formed rapidly without evidence for a compound I intermediate. Compound I must be formed, but its reaction to form compound II is rapid. This may be due to a degradation of the heme or a reaction with an amino acid side chain of the protein. The behavior of DHP and Y39F DHP in this regard is similar to that of myoglobin. Compound II is formed and appears to be stable for a number of minutes in solution. However, once compound II disappears the heme band shows a decrease in intensity indicating that degradation has occurred. Based on these observations, the time course for the spectra of DHP and Y39F indicates the intrinsic time constants for heme degradation. In the DHP PER SVD assay, v1 has a positive lobe at 413nm and v2 has a positive lobe at 420nm. The Y39F PER SVD plot shows that v2 has a positive lobe at 419nm and v1 has a positive lobe at 414nm. The H90G PER SVD plot shows that v2 has a positive lobe at 414nm and v1 has a positive lobe at 413nm. The peaks at 414nm are assumed to be the oxyferrous state of the heme.

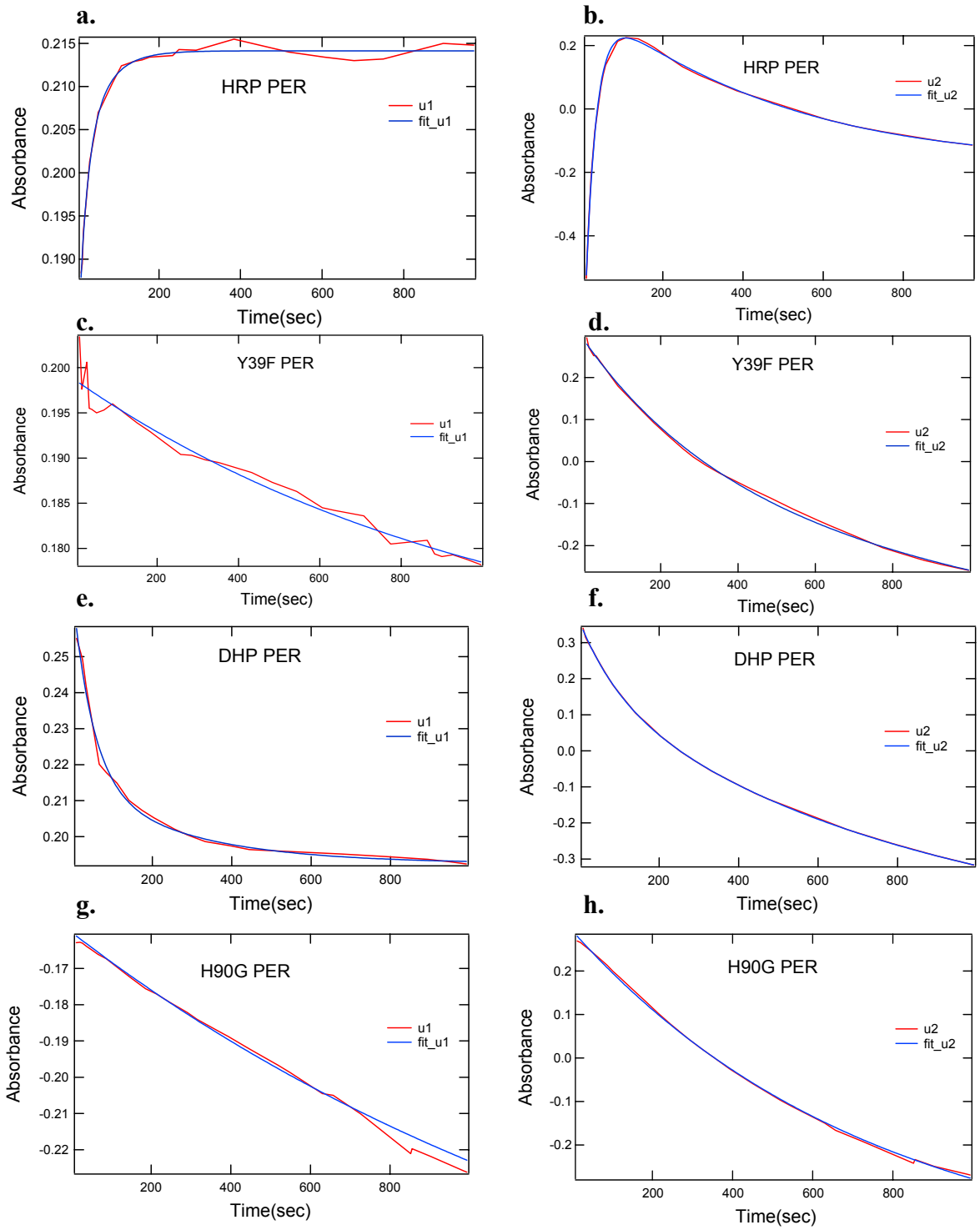

Figure 3.23 SVD Kinetics of Peroxide Degradation

3.4.6 Rate Constants

The time courses in Figs. 3.15, 3.17, 3.19, 3.21, 3.23 were fit to an exponential fitting function to determine the number of elementary processes that could possibly account for the data. The exponential equation used for non-linear least squares fitting is

$$Y(x)= a \exp(-k1x) + b \exp(-k2x) + c \exp(-k3x) + d \exp(-k4x)$$

The rate constants are reported in separate tables for each substrate. Depending on the number of components from one to four rate constants are reported in the table. Most of the TBP assay spectra fit to double exponentials as shown in table 3.2 above. The existence of multiple components may mean that there is more than one process occurring in the time courses t1 and t2. We will employ this hypothesis to attempt to explain the kinetics in terms of chemical processes such as consumption of substrate, formation of product and heme degradation by various mechanisms. The separation into processes helps to explain the components that are represented by t1 and t2. The main process represented by t2 is formation of product. Consumption of substrate and heme degradation are both represented in t1. However, t2 also has a very slow component that could be due to the product growth by a separate mechanism. HRP has a relatively equivalent rate constant for the two components (product growth and substrate consumption). On the other hand the kinetics of the t1 and t2 time courses of DHP are not matched indicating one of three possible differences with respect to DHP. A long-lived intermediate could be present in the protein binding pocket. A different product distribution could be produced (i.e. more polymeric product from one-electron oxidation and less quinone from two-electron oxidation). Finally, the heme degradation that is

apparent in time courses and fits above to peroxide-only data may be involved in the kinetics.

Tribromophenol Assay

	Offset	ΔA	k1	ΔA	k2
HRP,t1	2.588	2.298	0.0677		
HRP,t2	3.594	-5.115	0.0635		
Y39F,t1	4.197	0.800	0.0295	0.138	0.168
Y39F,t2	2.143	-1.312	0.0162	-0.866	0.0432
DHP,t1	3.536	0.550	0.0011	0.285	0.014
DHP,t2	1.777	-0.968	0.0056		

Table 3.2 Rate constants for rotated spectra of assays with TBP

Table 3.3 shows the rate constants for the assays with TCP and does not show the same phenomenon as the assay with TBP. DHP here has a slower rate of production than rate of substrate consumption. However, Y39F has the faster rate for product growth than for substrate consumption.

Trichlorophenol Assay

	Offset	ΔA	k1	ΔA	k2	ΔA	k3
Y39F,t1		3.931	0	1.432	0.026	0.791	0.002
Y39F,t2	6.1994	-3.069	0.019	-2.804	0.032		
DHP,t1	5.187	0.274	0.008	0.104	0.053		
DHP,t2	3.043	-1.954	0.0043	-0.429	0.02		

Table 3.3 Rate Constants for rotated spectra of assays with TCP

It was determined in this study that substrate concentration changes the effectiveness of the enzyme. By comparing table 3.3 and 3.4 the answers to whether the concentration of TCP affects DHP can be addressed. Table 3.4 shows that Y39F is slightly faster in t1 and t2 with less substrate which means that the rate constants for substrate consumption and product formation is greater when less substrate is present. On the other hand, DHP shows that t1 and t2 are slower meaning that substrate

consumption and product formation are slower when there is less substrate in the reaction. The observations that Y39F has larger rate constants and DHP has a smaller rate constant in the 49μM TCP assay gives clues that these two enzymes are very different in how they produce product. It is confirmed, though, that more product is made in the 82μM TCP assay by looking at the absorbance of the basis spectra for the product peak.

49μM Trichlorophenol Assay

	Offset	**ΔA**	**k1**	**ΔA**	**k2**	**ΔA**	**k3**
Y39F,t1		2.538	0	0.757	0.029	0.168	0.003
Y39F,t2	3.995	-3.331	0.022	-0.677	0.048		
DHP,t1		3.380	0	0.053	0.019	0.158	0.005
DHP,t2	2.166	-1.465	0.004	-0.173	0.017		

Table 3.4 Rate Constants for rotated spectra of assays with 49μM TCP

There are two rate constants for the t2 component of the Y39F TFP assay in table 3.5. However, the t1 component shows two fast components and one very slow component observed in DHP and Y39F enzymes. DHP has slower t2 components than Y39F. Y39F makes more product faster with less heme degradation.

Trifluorophenol Assay

	Offset	**ΔA**	**k1**	**ΔA**	**k2**	**ΔA**	**k3**
Y39F,t1		2.285	0	0.179	0.096	0.041	0.010
Y39F,t2	3.226	-1.049	0.002	-2.668	0.033		
DHP,t1	1.238	-0.174	0.002	-0.179	0.003		
DHP,t2		2.296	0.003	-2.461	0.006	0.247	0.003

Table 3.5 Rate Constants for rotated spectra of assays with TFP

Hydrogen Peroxide Assay

	Offset	ΔA	k1	ΔA	k2	ΔA	k3
HRP,u1		0.214	0	-0.0219	0.0506	-0.0145	0.0179
HRP,u2		-1.206	0.0373	2.728	0.00115	-2.382	0.000891
Y39F,u1	0.166	0.0327	0.000954				
Y39F,u2	-0.346	0.634	0.00194				
DHP,u1	-0.527	0.691	0.00120	0.195	0.00975		
DHP,u2	0.193	0.0229	0.00368	0.0514	0.0194		
H90G,u1	-0.297	0.137	0.000620				
H90G,u2	-0.482	0.775	0.00134				

Table 3.6 Rate Constants for SVD spectra with Hydrogen Peroxide

3.4.7 Normalized Plots

The theory that matter cannot be created nor destroyed is considered here when plots of the rotated rate spectra are normalized to 1. If substrate is directly formed into product than the sum of t1 and t2 should be close to 1. The rotated rate spectra (t1 and t2) for the TBP assay are plotted below. The t1 and t2 of each assay is plotted and normalized. If an enzyme is 1:1 for substrate consumption and product formation, then the sum of the normalized t1 and t2 should be 1. The normalized plots of HRP TBP in figure 3.24 show a tsum (t1 + t2) very close to one. However, the normalized plots of DHP TBP in figure 3.25 has a tsum above one. DHP appears to be producing a polymerized product or another product. In recent literature, HRP has been known to create the polymerized product and it is possible DHP is forming this product in a higher quantity according to the normalized plots.[3] Figure 3.26 shows the tsum below one for Y39F TBP. The product of Y39F is not known, but the plots give insight that it could be a radical intermediate. The rate constants correlated to the processes are also shown on these plots.

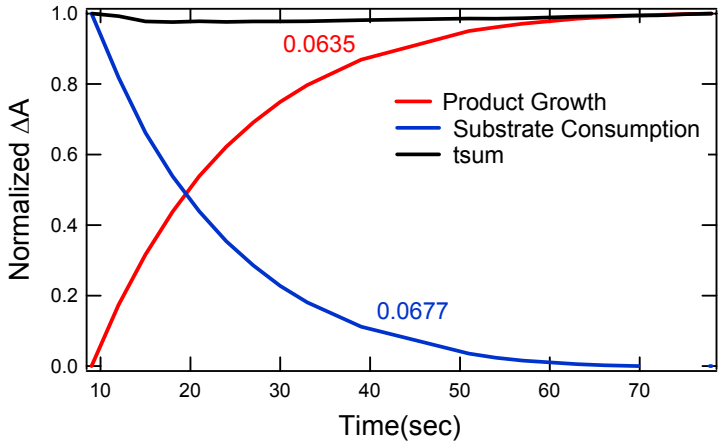

Figure 3.24 Normalized Plot of HRP TBP rates for product growth and substrate consumption

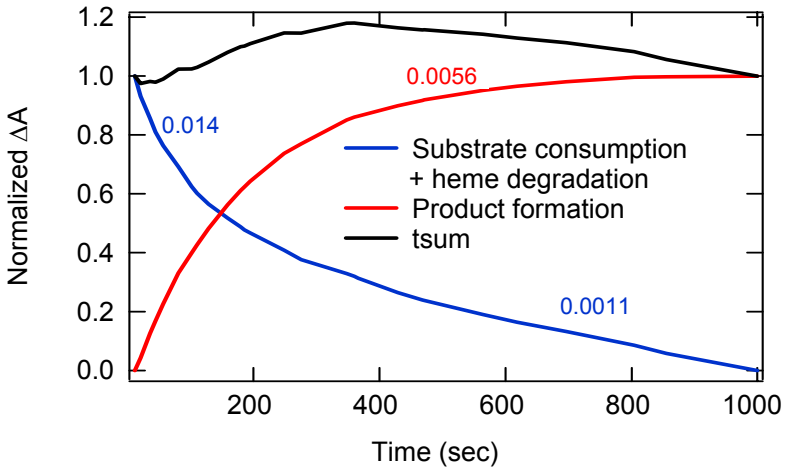

Figure 3.25 Normalized plot of DHP TBP rates for product growth and substrate consumption

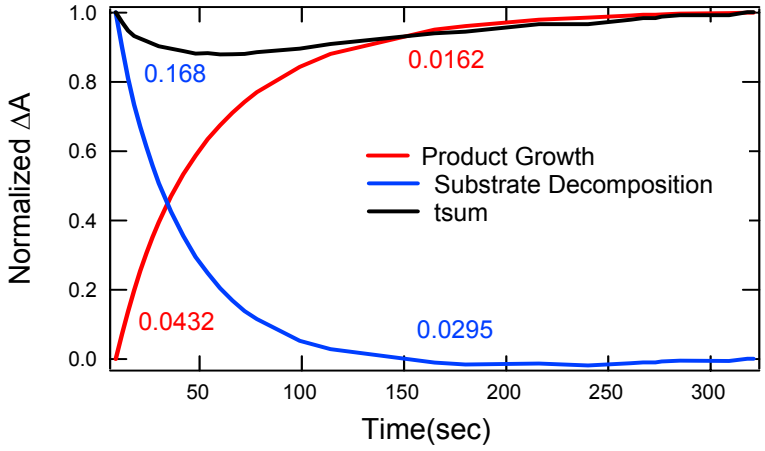

Figure 3.26 Normalized plot of Y39F TBP rates for product growth and substrate consumption

Normalized heme degradation rate plots from the basis spectra are shown below. These normalized plots are from the hydrogen peroxide assay with no substrate. It is shown that HRP increases fast in the beginning and then levels out indicating the formation of Compound II. It is also shown that Y39F decreases slower than DHP indicating that the heme degradation in Y39F is slower than DHP.

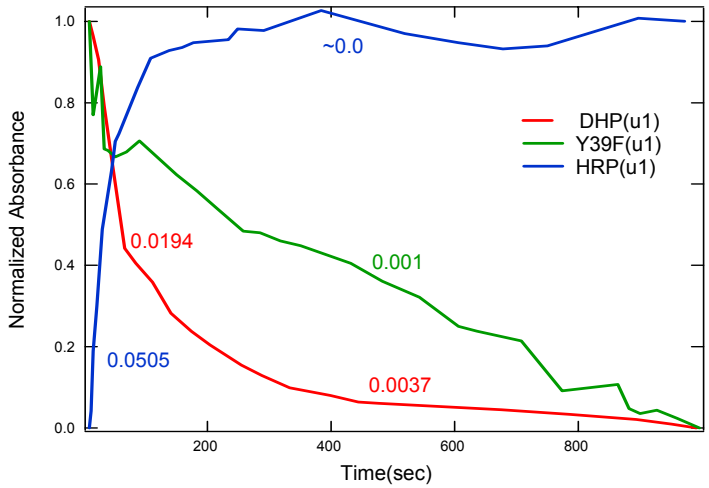

Figure 3.27 Normalized plot of heme degradation rates

3.4.8 Mechanistic Assumptions

The assumption that dehaloperoxidase uses peroxide as its cosubstrate is challenged in this study. The rate of heme degradation of DHP is substantially larger than that of HRP. In fact, in the data for HRP in the presence of peroxide presented in this thesis, the absorbance of the HRP Soret band increases over time. This increase (see Figure 3.27) is likely a result of the appearance of compound II. However, the DHP Soret band that corresponds to compound II decreases with a time constant of several minutes. The above analysis shows that if the absorbance decrease of the Soret band corresponds to heme degradation, the rate of heme degradation and substrate turnover are comparable in DHP. As a consequence of the apparent contradiction that degradation of

the heme and substrate consumption are on the same time scale, the proposed mechanism of DHP does not include a hydrogen peroxide as the cosubstrate, but rather an oxygen and an electron. Possibly since the heme is degraded by hydrogen peroxide, the native cosubstrate is oxygen.

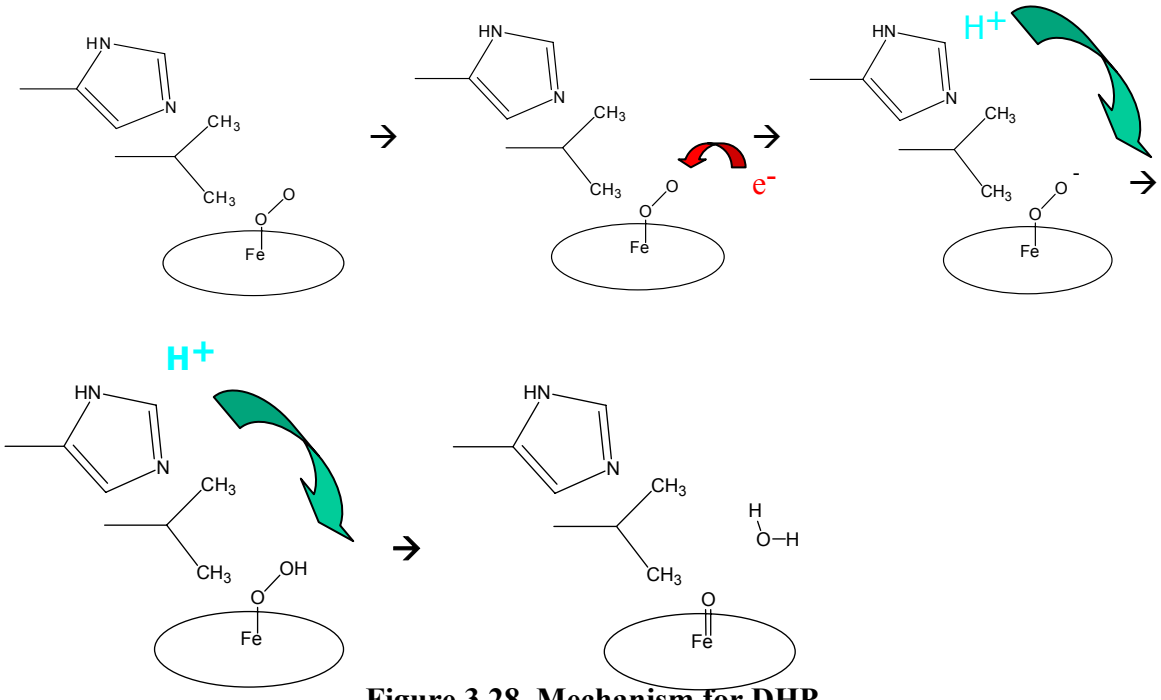

Figure 3.28 Mechanism for DHP

It is also proposed that the product of the DHP dehalogenating reaction includes a quinone and a polymerized product. These two products could both be formed by the reaction with a trihalogenated phenol.

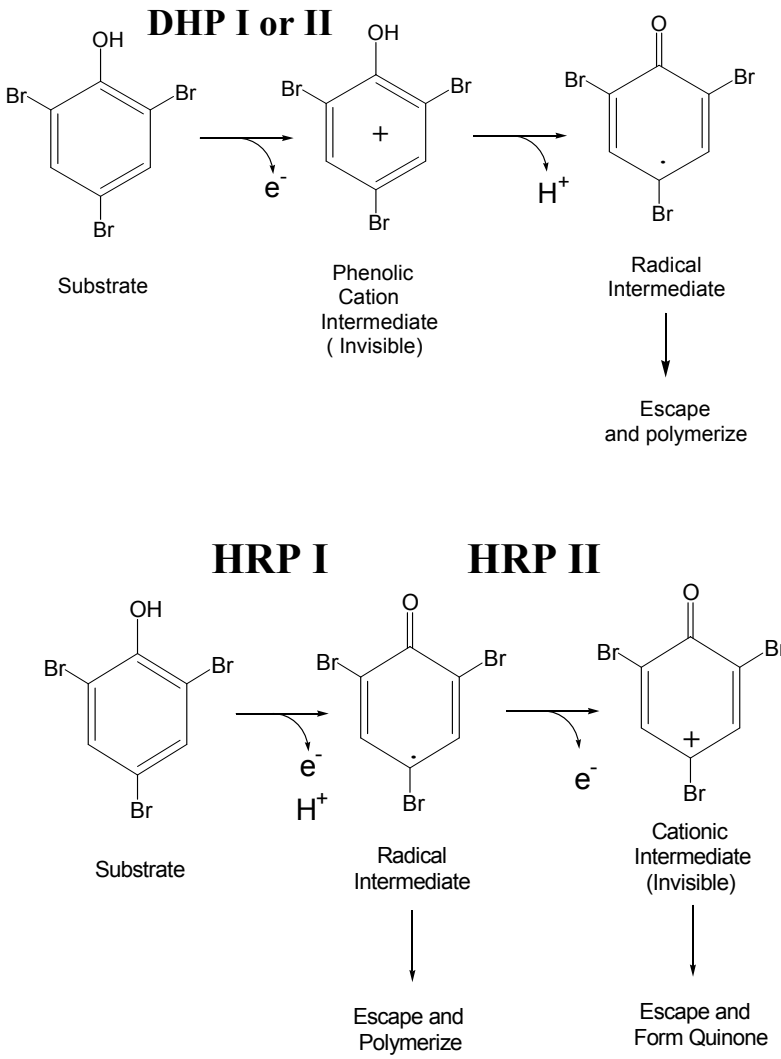

Figure 3.29 The one electron mechanism for HRP and DHP

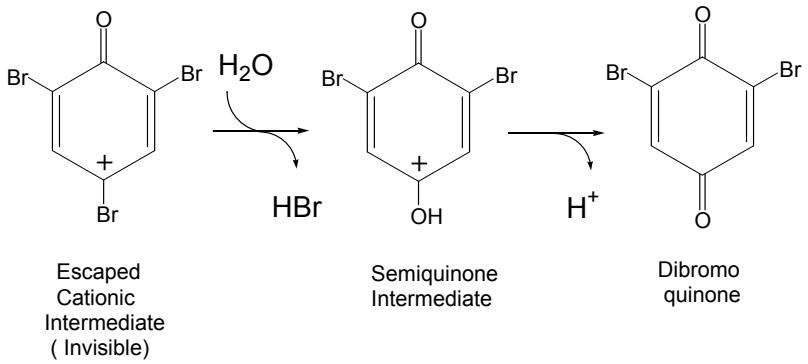

Figure 3.30 Mechanism forming quinone as product

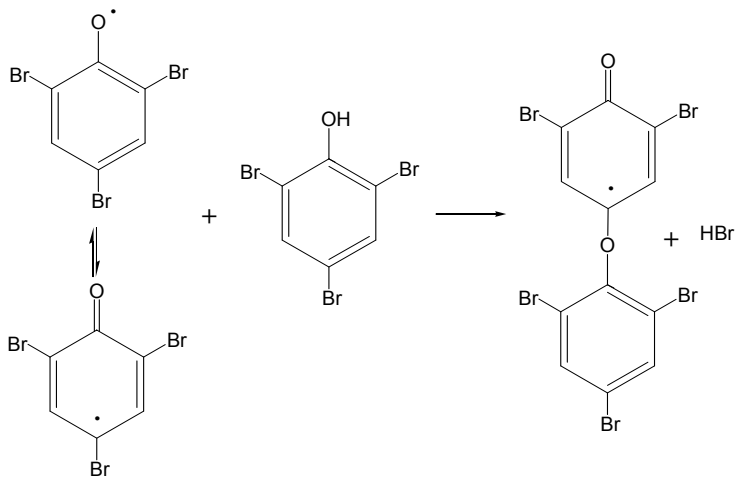

Figure 3.31 Mechanism forming the polymerized product

References:

[1] J. Belyea,M. Godek, C. Chaudhary, T. Sit, S. Lommel, J. Dawson, S. Franzen. Cloning, expression, purification and functional tests of a histidine-tagged dehaloperoxidase enzyme from Amphitrite ornata. *Manuscript in preparation*.

[2] Y. P. Chen, S. A. Woodin, D. E. Lincoln , C. R. Lovell. An unusual dehalogenating peroxidase from the marine terebellid polychaete *Amphitrite ornata.* *Journal of Biological Chemistry*, **1996** 271 (9): 4609-4612.

[3] M. L. Ferreira. UV/visible study of the reaction of oxidoreductases and model compounds with H2O2. *Macromolecular Bioscience*, **2003** 3 (3-4): 179-188.

Chapter 4: Conclusions

4.1 Conclusions

The mutant assays have shed light on the mechanism of the oxidation of the phenolic substrates by DHP. We consider first the mutation of the proximal an distal histidines, H90 and H56, respectively. H90G is a proximal histidine mutant that can be compared to H93G myoglobin or H175G cytochrome c peroxidase.[1-2] H90G shows no activity leading to the suggestion that the imidazole is an imidazolate by analogy with the situation in H175G CcP or at least that the role of the histidine is needed to stabilize the high oxidation state of the iron in compound I. Since H90 is an essential amino acid for the dehalogenating function of DHP, it is possible it is the 'push' in the 'push-pull' mechanism.

When histidine 56 was removed and replaced with an arginine, the activity of DHP was abolished. The location of H56 is not within hydrogen bonding distance of heme iron-bound peroxide or oxygen. The H56 residue is located one turn from the distal valine in DHP. Histidine 56 in DHP is 9.1Å from the heme, and the distal histidine in all peroxidases are ~5Å from the heme. Thus, H56 is positioned in a remote position relative to the heme in distinction to the distal histidines from other known peroxidases. In peroxidases, the histidine is providing a hydrogen bond with the iron which acts as the "pull" in the mechanism. It is hypothesized that H56 is providing the 'pull' in the 'push-pull' mechanism in DHP. However, the nature of the pull in the case of DHP is not the same pull in the Poulos-Kraut mechanism. In the Poulos-Kraut mechanism, the histidine is adjacent to the bound peroxide ligand and is capable of abstracting a hydrogen atom and redonating to promote O-O scission. In DHP the histidine can only act as a remote

proton shuttle. It was also shown in the assay analyses that DHP is less active than HRP and it is concluded that the position of this important histidine is partly responsible

Y39F activity is in between HRP and DHP, i.e. the rate of substrate oxidation is more rapid than that of DHP, but substantially slower than that of HRP. Based on the x-ray crystal structure, Y39 makes a hydrogen bond with the substrate, and by changing the tyrosine to a phenylalanine the enzymes turnover rate was increased. The mutation possibly opens the substrate binding pocket by removing an oxygen from the amino acid side chain, thus allowing product to be formed more readily.

Compound II is formed in DHP and HRP and is observed at 421nm. Compound II is formed in Y39F and is observed at 418nm. H90G and H56R heme peaks are at 414nm and do not shift, therefore, they do not create Compound II. Heme degradation and compound II formation are directly related to substrate decrease as shown in the SVD analysis in the r1 component spectra for all the enzymes studied. There is a biphasic decay of substrate that appears correlated with the loss of heme in DHP. The shift in the heme absorption band is likely due to formation of compound II from the resting state of the enzyme. It is likely that compound I is also formed but it is not observed because it reacts rapidly to form compound II.

The results of the present study suggest that DHP is not a peroxidase of the same type as HRP and Cyt C Peroxidase in that hydrogen peroxide is the cosubstrate. It likely binds oxygen in vivo and is then reduced by the known flavoprotein of DHP found in *Amphitrite ornata*.[3] This hypothesis is consistent with the greater rate of peroxide induced heme degradation in DHP than in HRP. The characteristic of DHP possibly makes it more like an oxygenase. For the purposes of bioremediation, it is proposed that

DHP may be better than other peroxidases because of its possible oxygen cosubstrate. Peroxide used in bioremediation may be harmful to the bacteria involved.

It is proposed that the radical intermediate of the substrate can either go on to form the quinone or escape from the protein and polymerize. This has been proven in DHP when the rate constants of substrate consumption and product growth do not match.

The normalized rate plots revealed more about DHP and Y39F. Y39F showed less heme degradation than DHP in figure 3.27 leading to the assumption that Y39F is a more efficient enzyme. If Y39F forms more product faster with less heme degradation, then it is a more efficient enzyme.

4.2 Future Research

There is much to be known about the mutants of DHP since they were developed for the first time in this study. Other mutants that affect the heme active site should be explored. Also, all of the mutants and HRP should be compared to the non-His tagged native DHP which was not available for these studies. It has been determined, though, that the six Histidines on DHP did not affect the reactivity. The mutants, H56R, H90G, and Y39F should be studied by IR spectroscopy with and without substrate bound. It would be useful to perform electron paramagnetic resonance (EPR) to find out more about the confirmation of the enzyme with and without substrate. Resonance Raman spectroscopy would be useful to perform on the mutants in oxy form and with CO bound.

References:

[1] M. W. LaCount, E. Zhang, Y. P. Chen, K. Han, M. M. Whitton, D. E. Lincoln, S. H. Woodin, and L. Lebioda. The Crystal Structure and Amino Acid Sequence of Dehaloperoxidase from *Amphitrite ornata* Indicate Common Ancestry with Globins. *J. Biol. Chem.* **2000**, *275*, 18712-18716.

[2] J. Sun, M. M. Fitzgerald, D. B. Goodin, and T. M. Loehr. The Solution and Crystal Structures of the H175G Mutant of Cytochrome c Peroxidase: A Resonance Raman Study. *J. Am. Chem. Soc.*, **1997**, 119, 2064.

[3] M. P. Roach, Y. P. Chen, S. A. Woodin, D. E. Lincoln, C. R. Lovell, J. H. Dawson Notomastus lobatus chloroperoxidase and Amphitrite ornata dehaloperoxidase both contain histidine as their proximal heme iron ligand. *Biochemistry* **1997,** 36, 8: 2197-2202.